land

MDPI

*Article*

# Modeling of Gully Erosion in Ethiopia as Influenced by Changes in Rainfall and Land Use Management Practices

**Tadesual Asamin Setargie [1,2,*], Atsushi Tsunekawa [3], Nigussie Haregeweyn [4], Mitsuru Tsubo [3], Mauro Rossi [5], Francesca Ardizzone [5], Matthias Vanmaercke [6], Sofie De Geeter [6], Ayele Almaw Fenta [4], Kindiye Ebabu [3,7], Mesenbet Yibeltal [2], Mulatu Liyew Berihun [2,8], Dagnenet Sultan [2], Benedict Nzioki [1] and Taye Minichil Meshesha [1,9]**

1 The United Graduate School of Agricultural Sciences, Tottori University, 4-101 Koyama-Minami, Tottori 680-8553, Japan
2 Faculty of Civil and Water Resources Engineering, Bahir Dar Institute of Technology, Bahir Dar University, Bahir Dar P.O. Box 26, Ethiopia
3 Arid Land Research Center, Tottori University, 1390 Hamasaka, Tottori 680-0001, Japan
4 International Platform for Dryland Research and Education, Tottori University, 1390 Hamasaka, Tottori 680-0001, Japan
5 National Research Council, Research Institute for Geo-Hydrological Protection, Via Della Madonna Alta126, 06128 Perugia, Italy
6 Department of Earth and Environmental Sciences, KU Leuven, Celestijnenlaan 200E, 3001 Heverlee, Belgium
7 College of Agriculture and Environmental Sciences, Bahir Dar University, Bahir Dar P.O. Box 1289, Ethiopia
8 Tropical Research and Education Center, University of Florida, Homestead, FL 33031, USA
9 Department of Hydraulic and Water Resources Engineering, Institute of Technology, Debre Markos University, Debre Markos P.O. Box 269, Ethiopia
* Correspondence: tadesual@gmail.com

**Abstract:** Gully erosion is one of the most extreme land degradation processes that exhibit spatial and temporal variation depending on topography, soil, climate, and land use and management characteristics. This study investigated the impact of changes in rainfall, land use/land cover (LULC), and land use management (LUM) practices on gully erosion in two midland watersheds (treated Kecha and untreated Laguna) in the Upper Blue Nile basin of Ethiopia by using the LANDPLANER model in combination with intensive field measurements and remote sensing products. We simulated gully erosion under past (in 2005), present (in 2021), and three potential future curve number conditions, each time under four rainfall scenarios (10, 30, 60, and 100 mm) using the dynamic erosion index (*e*), static topographic (*esp*), and erosion channel (*esp_channel*) thresholds. Density plot analyses showed that gullies frequently occur in low-lying gentle slope areas with relatively higher curve number values. The best predictions of gullies identified through true positive rates (TPR) and true negative rates (TNR) were achieved considering the static *esp_channel* > 1 for Kecha (TPR = 0.667 and TNR = 0.544) and the dynamic *e* > 0.1 for 60 mm of rainfall in Laguna (TPR = 0.769 and TNR = 0.516). Despite the 10 mm rainfall having negligible erosion-triggering potential in both watersheds, the 60 and 100 mm rainfall scenarios were 4–5 and 10–17 times, respectively, higher than the 30 mm rainfall scenario. While the LULC change in the untreated Laguna watershed increased the impact of rainfall on gully initiation by only 0–2% between 2005 and 2021, the combination of LULC and LUM significantly reduced the impact of rainfall in the treated Kecha watershed by 64–79%. Similarly, the gully initiation area in Kecha was reduced by 28% (from 33% in 2005 to 5% in 2021) due to changes in LULC and LUM practices, whereas Laguna showed little increment by only 1% (from 42% in 2005 to 43% in 2021) due to LULC change. In addition, the future predicted alternative land use planning options showed that gully initiation areas in Laguna could be reduced by 1% with only LULC conversion; 39% when only LUM practices were implemented; and 37% when both were combined. These results indicate that LUM practices outweigh the impact of LULC on gully erosion in the studied paired watersheds. Overall, LANDPLANER successfully simulated the spatio-temporal variation of gully erosion with scenario-based analyses and hence can be used to predict gullies in the study area and other data-scarce regions with similar agro-ecological settings.



**Citation:** Setargie, T.A.; Tsunekawa, A.; Haregeweyn, N.; Tsubo, M.; Rossi, M.; Ardizzone, F.; Vanmaercke, M.; De Geeter, S.; Fenta, A.A.; Ebabu, K.; et al. Modeling of Gully Erosion in Ethiopia as Influenced by Changes in Rainfall and Land Use Management Practices. *Land* **2023**, *12*, 947. https://doi.org/10.3390/land12050947

Academic Editor: Zhi-Hua Shi

Received: 26 March 2023
Revised: 11 April 2023
Accepted: 13 April 2023
Published: 24 April 2023

**Keywords:** LANDPLANER; topographic threshold; GIS and RS; sustainable land management; land use/land cover; runoff curve number; dryland

## 1. Introduction

Gully erosion is one of the most extreme land surface processes in many regions. Yet, its extent and spatio-temporal distributions are affected by the dynamic interaction of several environmental factors. Despite gullies having no clear-cut upper limit boundaries and that their width and depth could extend to hundreds of meters [1], they are considered to have a tillage irreversible minimum depth of about 0.5 m [2], a width of one foot or ~0.3 m [3], and a cross-sectional area of one square foot or ~929 $cm^2$ [4]. Once the initiation of gullies starts, the upslope expansion of gullies mainly happens through the retreat of active headcuts, called gully heads. Gully headcuts show a marked drop in elevation compared to the gully channel bed [5]. Gullies can have various on-site and off-site environmental impacts, including loss of land, damage to infrastructures, and sometimes casualties [6].

Studies show that topography, soil, climate, and land use/land cover (LULC) can strongly affect the occurrence and distribution of gullies [1,6–8]. The topographic and soil-related factors are known to have a relatively static influence, while the climate and LULC-related factors have a dynamic effect on the initiation and expansion of gullies [9,10]. Thus, changes in LULC and climatic elements such as rainfall can highly influence the initiation and relative position of gully heads and, hence, define the spatio-temporal extent of gullies across different climatic regions. A study conducted in the Mediterranean environment of Spain showed that gully heads were best correlated with rainy day normal, a long-term average depth of rainfall on rainy days, while rainfall and LULC have primary and secondary controls over gully heads [11]. Vanmaercke et al. [5] confirmed that gully heads globally showed sensitivity to rainfall intensities and could retreat extremely fast with up to 135 m $yr^{-1}$, 3628 $m^2$ $yr^{-1}$, and 430 $m^3$ $yr^{-1}$ regarding linear, areal, and volumetric retreat rates, respectively. The study also reported that the volumetric retreat rates were significantly correlated with a rainy day normal and may increase by 200–300% if rainfall intensities increase by the expected 10–15% due to climate change [5]. Amare et al. [12] also reported that the amount of rainfall influences the retreat rate of valley bottom gullies. Similar studies conducted across humid and sub-humid environments of the Upper Blue Nile basin in Ethiopia showed that the rainfall-induced rise in the groundwater table [13–15] and land use management (LUM) (e.g., [16,17]) could also influence the retreat rates and the modeling of gully erosion. It was also reported that LULC and LUM practices could influence the spatio-temporal evolution of gully erosion globally [7]. However, there is still a gap in studying the separate and combined effect of changes in rainfall, LULC, and LUM practices on gully erosion.

Several modeling approaches with different specific purposes and input data requirements have been used to assess gully erosion in the past decades. Process-based gully erosion models consider the actual physical processes in a conceptually transparent approach, but their applicability is limited to small areas where they are derived and often have large data requirements for calibration and validation purposes [18–20]. On the other hand, empirical (e.g., statistical and machine learning) approaches can give meaningful estimates with minimal assumptions and fewer data requirements [6]. However, despite their robust predictions, the direct interpretation of machine learning-predicted results can be difficult due to the lack of an explicit model [21]. Setargie et al. [17] employed a Random Forest-based machine learning approach and revealed that runoff curve number and LULC were among the top controlling factors that determine the spatial distribution of gullies in the current study area. However, the effect of rainfall was not investigated in the previous study, as it has been assumed homogeneous within the studied small watersheds [22]. In addition to changes in rainfall and LULC, scenario-based assessments of gully erosion may be required to model the effect of the adapted and future implemented LUM practices in

the watersheds. Thus, to completely understand the spatio-temporal dynamics of gully erosion in the study area, the impact of variations in rainfall, LULC, and LUM practices need to be further investigated.

In this study, a simplified distributed rainfall-runoff model called the LANDPLANER (LANDscape, Plants, LANdslide, and Erosion) model was employed to investigate the impact of changes in rainfall, LULC, and LUM practices on gully erosion modeling. The model is a distributed model and is capable of simulating the dynamic response of watersheds for gully initiation under a changing climate and LULC and LUM scenarios in a simplified process-oriented way that corresponds with our understanding of the gully erosion [23,24]. LANDPLANER was selected in this study for three main reasons. First, the model predicts the location of gullies and gully heads using a curve number-based approach, which was identified as an important factor of gully erosion in the literature [25,26] and in our previous study conducted in the study area [17]. Second, the model can simulate the impact of changing rainfall considering the threshold-dependent nature of gullies [25,27] that would otherwise be impossible to account for the variability of rainfall in small watersheds. Third, the applicability of the model was priorly tested in two study areas. The model was tested in dryland and Mediterranean environments across Iran and Italy [6], respectively, considering gullies as point and line features [9,10]. Thus, this study is the first case to apply the model in a sub-humid climate in the tropical region of Africa representing gullies by point and polygon features.

We evaluated the separate and combined impacts of rainfall, LULC, and LUM practices on gully erosion with single and paired watershed approaches. The single watershed approach (e.g., [28–30]) compared the model simulated results before and after changes in each watershed, while the paired watershed approach (e.g., [31–33]) compared the results before and after changes across different watersheds. Even though the impacts of rainfall, LULC, or LUM practices were investigated in a few gully erosion studies (e.g., [11,34,35]), to our knowledge, the separate and combined impacts were not examined using single and paired watershed approaches. The objectives of this study were therefore to (1) characterize gullies with input datasets of the model ahead of running the model, (2) test the potential of LANDPLANER to predict the location of gullies based on the static and dynamic thresholds of the model, and (3) conduct scenario-based analyses to model the impact of changes in rainfall, LULC, and LUM practices on the spatio-temporal variation of gully erosion.

## 2. Study Area

The study was carried out in adjacent paired watersheds (Kecha and Laguna), separated by a common drainage divide, at the Aba Gerima site representing a midland agro-ecology of the Upper Blue Nile basin in Ethiopia (Figure 1). The paired watersheds were selected by design to evaluate the impact of LUM practices on gullies found across the watersheds. While there was no LUM practice in Laguna in the past (2005) and present (2021), Kecha has been part of the National Sustainable Land Management Program since 2011 [33]. The cultivated lands in Kecha are terraced, and the grazing and bushlands are protected compared to Laguna. Hence, Kecha represents a treated condition with LUM practices, while Laguna represents an untreated condition. Terraces, soil, and stone bunds are widely employed land management practices in Kecha [33]. The elevation in Kecha and Laguna varies between 1913 and 2122 and 1946 and 2253 m.a.s.l., while their slope gradients vary between 0 and 89 and 0 and 133%, with mean values of 14% and 27%, respectively. The long-term (1962–2020) mean annual rainfall of the site recorded at the nearest Bahir Dar meteorological station is 1450 mm while the average daily temperature is about 20 °C. The study site has a sub-humid (moist *Weyna Dega*) climate based on the classification of Hurni et al. [36]. The study watersheds share similar characteristics in terms of altitude, rainfall, temperature, and major crops except for differences in topographical settings and the coverage of LUM practices (Table S1). They are highly vulnerable to gully erosion due to human activities and climate variability [16,17]. In Kecha, 32 gullies were mapped in 2005 and increased to 37 gullies in 2021, whereas gullies in Laguna were 13 in 2005 and

increased to 24 in 2021. The locations of gullies were further confirmed during recent field observations conducted from August to September 2022. A detailed description of gullies and the paired watersheds is given in Setargie et al. [17].

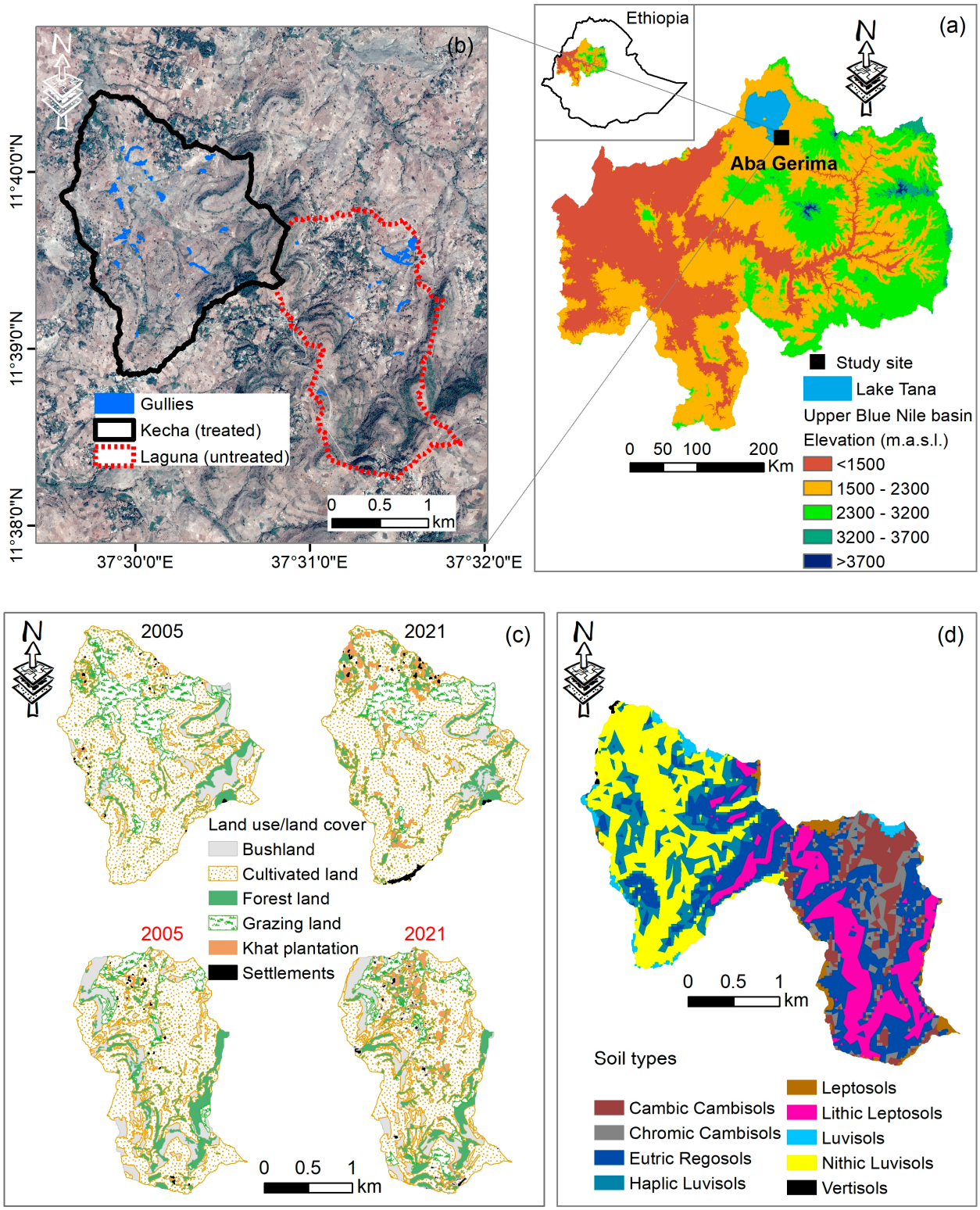


**Figure 1.** (**a**) Location of the study site (Aba Gerima) in the Upper Blue Nile basin in Ethiopia, (**b**) gullies in the paired Kecha and Laguna watersheds, (**c**) the LULC maps of the watersheds for the years 2005 and 2021, and (**d**) the soil maps [37] of watersheds.

## 3. Methodology

### *3.1. LANDPLANER Model*

In this study, the LANDPLANER model was employed to evaluate the impact of changes in rainfall, LULC, and LUM on gully erosion beyond testing the applicability of the model in the study area. LANDPLANDER is an integrated hydrological, erosion, and landslide model developed to simulate the effect of changing climate, land use, and hillslope topography on the triggering/occurrence of erosion and landslide phenomena [23]. It aimed to evaluate the dynamic response of watersheds for gully occurrences under different rainfall and curve number scenarios [24]. It is an open-source raster-based distributed model written in R programming language [38]. The model performs pixel-based analyses with spatial input and output data provided in standard geographical '*.asc*' format. The modeling schema of LANDPLANER allows for the computation of erosion indices and topographic thresholds, taking input from its rainfall-runoff hydrological modules.

#### 3.1.1. Hydrological Modeling

The hydrological model considers rainfall, runoff, infiltration, exfiltration, evaporation, and transpiration for water repartition, while it uses a modified runoff curve number approach [23,24] to estimate the surface runoff. The runoff curve number (CN), developed by the former Soil Conservation Service (SCS) of the United States Department of Agriculture (USDA), is an empirical parameter used to calculate direct runoff from excess rainfall based on the hydrologic soil-cover complexes of the area [39]. Unlike the original CN approach where runoff is computed based on a weighted average CN assigned for the whole basin [39], this model adds the upslope generated runoff to each downslope draining cell of the basin (Equation (1)):

$$Q_{off} = \frac{(P + \sum Q_{on} - \lambda S)^2}{P + \sum Q_{on} + (1 - \lambda)S} \quad (1)$$

where $Q_{off}$ is the runoff towards the downslope cell (in), $P$ is the depth of rainfall (in), $Q_{on}$ is the runoff from the upslope cell (in), $\lambda$ is the initial abstraction ratio (dimensionless), and $S$ is the maximum potential retention (in). $Q_{off}$, $P$, and $Q_{on}$ are computed on a daily basis, while $S_{0.05}$ was used for an initial abstraction of 5% (i.e., $\lambda = 0.05S$).

A study by Hawkins et al. [40] suggested that the use of $S_{0.05}$ (i.e., $\lambda = 0.05S$) as shown in Equation (2) might be more appropriate than the original $S_{0.2}$ (i.e., $\lambda = 0.2S$) relationship derived by SCS [39]:

$$S_{0.05} = 25.4 \cdot 1.33 \left[ \frac{1000}{CN} - 10 \right]^{1.15} \quad (2)$$

where $CN$ is the curve number (dimensionless), and $S_{0.05}$ is the maximum potential retention (mm). A normal antecedent moisture condition (i.e., AMC II) was assumed to calculate the associated runoff curve number-II (CN2) in the study watersheds.

#### 3.1.2. Erosion Index

The dynamic erosion index ($e$) indicates the stream power of direct runoff on the land surface and is used to model the erosion-triggering potential of surface runoff. Detailed investigations on the local rainfall, slope, soil, and LULC and LUM characteristics are necessary to model the dynamic erosion process using the hydrologic model. Hence, Rossi [23] introduced a potential erosion index (Equation (3)), which is further simplified into an expected erosion index (Equation (4)), to identify the potential hotspot areas of erosion:

$$e_{pot} = \alpha \cdot \left( \frac{Q_{off} \cdot \sin(s)}{S_{0.05}} \right)^{\beta} \quad (3)$$

$$e = \frac{Q_{off} \cdot \sin(s)}{S_{0.05}} \quad (4)$$

where $e_{pot}$ and $e$ are potential and expected erosion indices (dimensionless), $Q_{off}$ is the cell runoff calculated by the hydrological model (mm), $s$ is slope angle (degree), $\alpha$ and $\beta$ are coefficients (dimensionless) assumed unity unless calibration is made, and $S_{0.05}$ (mm) is given in Equation (2).

#### 3.1.3. Topographic Thresholds

The physical-based topographic gully head threshold equation proposed by Torri and Poesen [25], as shown in Equation (5), is used to locate gully heads exceeding the topographic threshold (*esp*) of the area:

$$\sin(s) \geq 0.73ce^{1.3RFC}(0.00124 \cdot S_{0.05} - 0.037)A^{-0.38} \quad (5)$$

where $s$ is the slope angle (degree), $c$ is a correction coefficient (dimensionless) to represent unaccounted sources of variation (assumed unity), $RFC$ is surface rock fragment cover (%), $S_{0.05}$ (mm) is given in Equation (2), and $A$ is an upslope contributing area (ha). For the gully head to initiate, the above equation must exceed its critical threshold. The *esp* marks gully initiation points based on the topographic threshold approach [25], while the *erosion_channel* defines erosion channels downslope of the gully initiation points, which marks potential areas of gullies [23].

Although the standard formulation of the topographic threshold model is considered static as it does not directly depend on rainfall and generated runoff [9,23], LANDPLANER considers the dynamic effects of changing rainfall and LULC on gully erosion by considering different scenarios of rainfall and LULC [24].

### *3.2. Preparation and Characterization of Model Input Data*

Before running LANDPLANER, the geomorphic input variables of the model (i.e., elevation, slope, flow direction, and flow accumulation) and the curve number maps were analyzed using density plot analysis. The density plot analysis helped to show the distribution of gully and non-gully areas based on the probability density function of the input variables of the model [9,26].

The spatial input datasets were extracted from a very high resolution (5 m × 5 m) digital elevation model (DEM) map aggregated from a high-accuracy 0.5-m ALOS World 3D Enhanced DEM (https://www.aw3d.jp/en/products/enhanced/, accessed on 14 March 2023), high-resolution (QuickBird and Pleiades) satellite images, and local soil maps created by means of intensive fieldwork and laboratory analyses [37]. The DEM-derived morphological input variables of the model were elevation, slope, flow direction, and flow accumulation maps. Using the LULC maps (Figure 1c; Table S2) manually digitized from the high-resolution satellite images taken in 2005 and 2021, together with detailed soil maps of the areas (Figure 1d; Table S3), the curve number maps were produced for the past (i.e., $CN_{2005}$) and present (i.e., $CN_{2021}$) scenarios using the associated hydrologic soil-cover complexes (i.e., hydrologic soil groups, land uses, and treatment classes; see Table S4) [39]. All the spatial input datasets were analyzed and prepared (in standard geographical '*.asc*' format) in ArcGIS Pro [41] and GRASS GIS [42] environments, while LANDPLANER was run in the R environment [38].

### *3.3. Validation of Model Prediction Performance*

The prediction performance of the model was validated using statistical metrics, and the best-performing scenarios were identified for use in predicting the location of gullies in the study watersheds. The gully inventory maps were prepared by digitizing a total of 126 gullies from satellite images taken in 2005 and 2021 (see Table 1).

**Table 1.** Details of the satellite images used to construct the gully inventory maps.

| Study Site | Satellite Sensor | Spectral Resolution | Spatial Resolution (m) | Acquisition Date (Day Month Year) |
|---|---|---|---|---|
| Aba Gerima | QuickBird | Multispectral | 0.6 × 0.6 | 6 March 2005 |
| | Pleiades | Multispectral | 0.5 × 0.5 | 7 January 2021 |

The performance metrics of gully head and erosion channel predictions were evaluated based on the dynamic erosion indices (*e*) and the static topographic (*esp*) and erosion channel (*esp_channel*) threshold outputs of the LANDPLANER model. The predicted *esp* are binary results that can be directly used to validate the presence of gully heads, while certain critical thresholds needed to be assumed for the continuous *e* and *esp_channel* variables to validate their predictions of gullies. The critical thresholds of erosion indices (*e*) exceeding 0.01, 0.05, 0.1, 0.5, 1, 5, and 10 were used to evaluate the occurrence of gullies depending on the curve number and rainfall scenarios, while an erosion channel (*esp_channel*) exceeding 1 was assumed to validate gullies. Although the erosion index (*e*) was designed to show the erosion potential (Equation (3); [23]) and needs calibration to directly convert into (gully) erosion amount, it can also be used to predict the location of gullies [9,10].

The statistical accuracy metrics used to evaluate the agreement between model prediction and observed gullies in the study areas made use of true positive (TP), true negative (TN), false positive (FP), and false negative (FN) values. The additional derived metrics included true positive rate or sensitivity (Equation (6)), true negative rate or specificity (Equation (7)), and overall accuracy or efficiency (Equation (8)).

$$TPR = \frac{TP}{TP + FN} \tag{6}$$

$$TNR = \frac{TN}{TN + FP} \tag{7}$$

$$OA = \frac{TP + TN}{TP + TN + FP + FN} \tag{8}$$

The TP and TN values count the correctly predicted gullied and non-gullied pixels whereas, and the FP and FN values count the wrongly classified gullied and non-gullied pixels, respectively. On the other hand, the TPR and TNR values show the contribution of correctly predicted gullied and non-gullied pixels relative to the entire observed gully and non-gully areas, respectively. Similarly, the FPR and FNR values indicate the proportion of wrongly classified gullied and non-gullied pixels relative to the total observed gully and non-gully areas, respectively. Hence, the higher the TPR and TNR value, the better the predicted performance. On the contrary, the prediction performance decrease as FPR and FNR values increase. Since a good predicting model needs to have a higher TPR and TNR values, the predicted results were compared by their jointly maximized values (i.e., an average of TPR and TNR) to select the best-performing scenarios [10]. The 'caret' and 'ggplot2' packages in R were used for the accuracy assessment of predicted results and the presentation of analysis results, respectively.

### *3.4. Assessing the Impact of Rainfall, LULC, and LUM Practices on Gully Erosion*

Five curve number scenarios were considered to evaluate the impact of changes in rainfall, LULC, and LUM practices on the spatio-temporal modeling of gully erosion. The past ($CN_{2005}$) and present ($CN_{2021}$) curve number scenarios were prepared using the oldest (2005) and latest (2021) high-resolution satellite images available (Table 1) to show the impact of LULC and LUM practices in the study area. In addition, three future curve number scenarios ($CN_{option1}$, $CN_{option2}$, and $CN_{option3}$) prepared based on alternative land use planning options were used to assess the impact of LULC changes and LUM practices on gully initiation. The $CN_{option1}$, $CN_{option2}$, and $CN_{option3}$ scenarios assessed the effect of

proposed changes in LULC, LUM, and LULC and LUM, respectively, on gully initiation in Laguna. These alternative land use planning options, adapted from the national integrated local level land use planning manual prepared by the Ministry of Agriculture (MoA) of The Federal Democratic Republic of Ethiopia (FDRE), were developed based on a simple and less-expensive land use planning method called land capability classification [43].

Similarly, four event-based rainfall scenarios of 10, 30, 60, and 100 mm were considered based on a literature review. These critical rainfall thresholds are potentially capable of triggering rills and (ephemeral) gullies worldwide [1,18] and are plausible values for the studied watersheds. A daily rainfall depth of 7.5–20 mm was needed to initiate rills in croplands [44,45], 15–18 mm to initiate ephemeral gullies in croplands [46], and 80–100 mm to initiate gullies in forest land [47]. The locations of gullies were predicted by the model for four rainfall scenarios (i.e., 10, 30, 60, and 100 mm) under two curve number scenarios (i.e., $CN_{2005}$ and $CN_{2021}$) for Kecha and under five curve number scenarios (i.e., $CN_{2005}$, $CN_{2021}$, $CN_{option1}$, $CN_{option2}$, and $CN_{option3}$) for Laguna. Hence, a total of 8 and 20 simulations were run for Kecha and Laguna watersheds, respectively. Figure 2 presents the detailed methodological flowchart followed in this study.

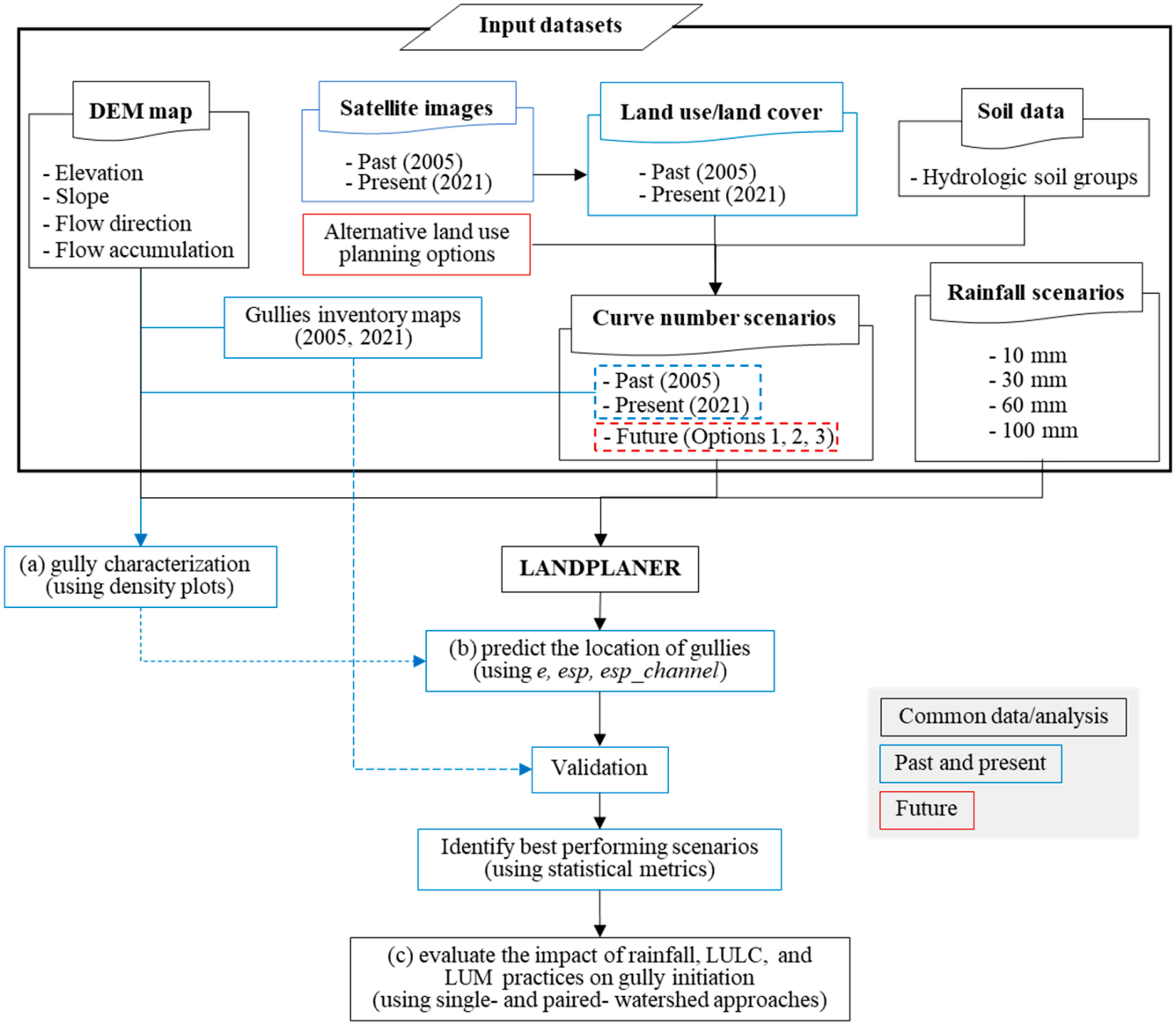


**Figure 2.** Methodological flowchart followed in this study. Refer to Sections 1 and 3.1 for abbreviations.

The separate and combined impacts of changes in rainfall, LULC, and LUM treatment conditions in the study watersheds between 2005 and 2021 were evaluated using single and paired watershed approaches [33]. Although Laguna remains untreated in the past (i.e., 2005) and present (i.e., 2021), Kecha was treated since 2011. The paired watershed approach compared differences in the predicted gully initiation areas between the treated (Kecha) and untreated (Laguna) watersheds, while the single watershed approach compared the separate and combined impact of rainfall, LULC, and LUM practices in each watershed. In addition to the past and present scenarios, three alternative land use planning options were formulated to evaluate the separate and combined influence of LULC and LUM practices on future gully initiation based on the MoA FDRE [43] guidelines. The first option ($CN_{option1}$) recommended LULC conversion by avoiding crop cultivation on steep slopes (>30%) and afforesting hillslope (>50%) areas without implementing any LUM practices. The second option ($CN_{option2}$) recommended the implementation of different LUM practices extensively monitored across 42 field plots in three experimental sites in the Upper Blue Nile basin. The third option ($CN_{option3}$) recommended both the conversion of LULC and the implementation of LUM practices. The LUM treatment options were 'bund+grass' for cultivated lands, 'enclosure' for grazing lands, 'trench+enclosure' for bushlands, and 'napier+desmodium' for khat plantations. The validated curve number values of these LUM options [30] were used to evaluate their impact on gully initiation in Laguna.

## 4. Results

### *4.1. Characterizing Gully Erosion with Model Input Variables*

The input variables of the model in both watersheds exhibited spatial (Figure 3a–h) and spatio-temporal variations (Figure 4a–d).

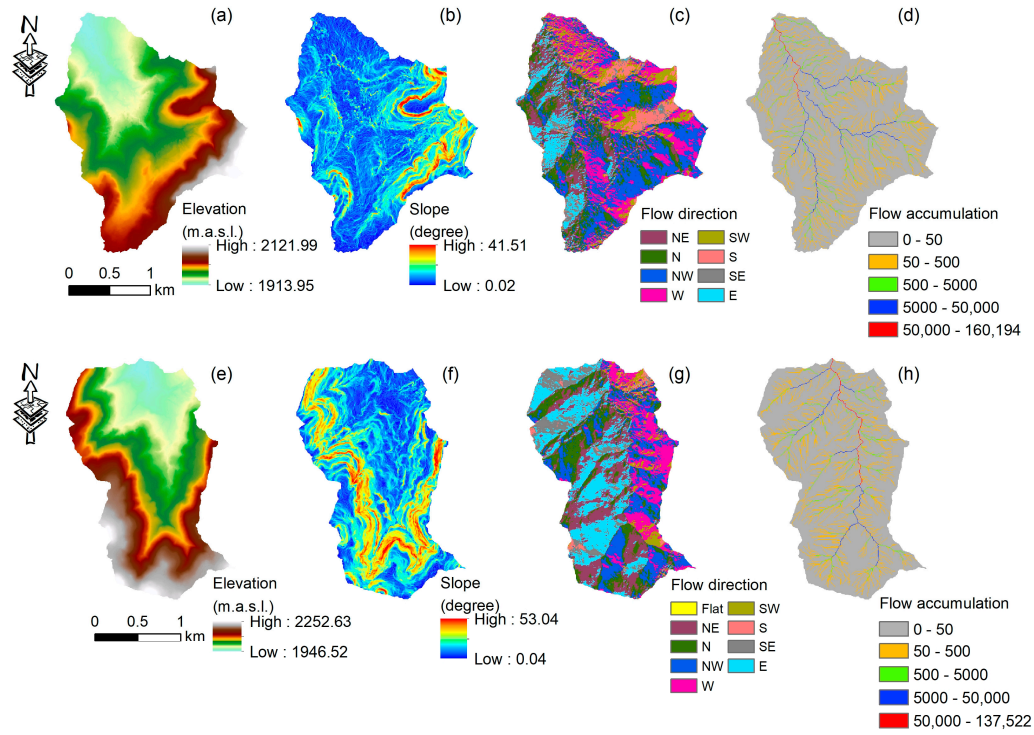


**Figure 3.** Maps of DEM-derived input variables of the LANDPLANER model for Kecha (top panel, **a**–**d**) and Laguna (bottom panel, **e**–**h**) watersheds: (**a**,**e**) elevation, (**b**,**f**) slope, (**c**,**g**) flow direction, and (**d**,**h**) flow accumulation. NE: north-east; N: north; NW: north-west; W: west; SW: south-west; S: south; SE: south-east; E: east.

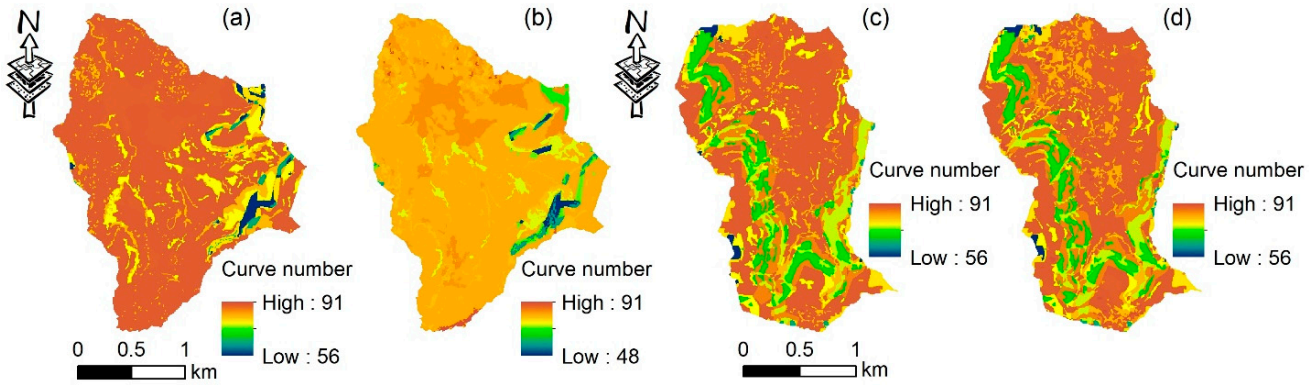


**Figure 4.** Maps of different curve number scenarios: (**a**) Kecha in 2005, (**b**) Kecha in 2021, (**c**) Laguna in 2005, and (**d**) Laguna in 2021. See Table S4a–d for the derivation of runoff curve number-II.

The density plots of elevation showed that gullies in both watersheds were frequently found in the low-lying areas around 1935–1970 m.a.s.l. (Kecha) and 1975–2005 m.a.s.l. (Laguna) relative to hillslope areas (Figure 5a,f,k,p). Most of the gullies in Laguna were concentrated in the lowland areas, except for little presence in the hillslope areas compared to Kecha, which showed more distribution of gullies over the watershed area. Most gullies at both watersheds were found in gentle slopes between 5 and 20°, with gullies at Laguna having slightly higher slopes compared to Kecha (higher modal value in Figure 5b,g,l,q). In addition, most gullies in both watersheds were found on NW-facing slopes, with Laguna showing a clear distinction, while most non-gully areas in Kecha and Laguna were on NW- and E-facing slopes, respectively (Figure 5c,h,m,r). Both gully and non-gully areas exist in low and high flow accumulation areas, which makes it difficult to differentiate gullies just by looking at the flow accumulation frequency density maps (Figure 5d,i,n,s). Gullies showed preference towards the higher curve number values, primarily around 90 (in 2005) and between 81 and 84 (in 2021) for Kecha and around 90 (in 2005 and 2021) for Laguna (Figure 5e). The higher numbers corresponded with cultivated and grazing lands in high-clay soils. Conversely, the higher density of non-gullied areas was concentrated around the same curve number values, while it was overlaid with gullied areas. The response of input factors of the model showed a similar trend for the past and present conditions of gullies in the study watersheds, despite the expansion and addition of new gullies (Figure 5).

### *4.2. Evaluating Dynamic and Static Thresholds for Different Rainfall and Curve Number Scenarios*

#### 4.2.1. Performance of Erosion Index (e) Thresholds for Different Curve Number and Rainfall Scenarios

LANDPLANER predicted the potential locations of gullies through erosion indices (*e*) for the considered curve number ($CN_{2005}$, $CN_{2021}$) and rainfall (10, 30, 60, 100 mm) scenarios (Figure 6a–p). The maximum erosion indices with the highest erosion potential corresponding to rainfall magnitudes of 10, 30, 60, and 100 mm in 2005 were 0.05, 1.37, 8.78, and 28.45 for Kecha and 0.06, 2.29, 17.44, and 48.73 for Laguna, respectively (Table S5). These maximum values of erosion indices increased to 0.01, 0.24, 2.36, and 12.57 in Kecha and to 0.06, 2.25, 13.03, and 53.82 in Laguna, corresponding to the rainfall amounts of 10, 30, 60, and 100 mm in 2021, respectively (Table S5). As expected, the average and maximum erosion indices showed an increasing trend with increasing runoff due to an increase in the magnitude of rainfall (see Equations (1) and (4)), with the maximum values found for 100 mm of rainfall for both curve number scenarios in both watersheds. The average and maximum erosion indices for $CN_{2021}$ were also slightly higher than that of $CN_{2005}$ for the same rainfall magnitudes. Laguna was found to have relatively higher average and maximum erosion indices compared to Kecha under similar curve number and rainfall

conditions (Table S5). The erosion hotspot areas in both watersheds were highlighted by higher erosion indices (Figure 6).

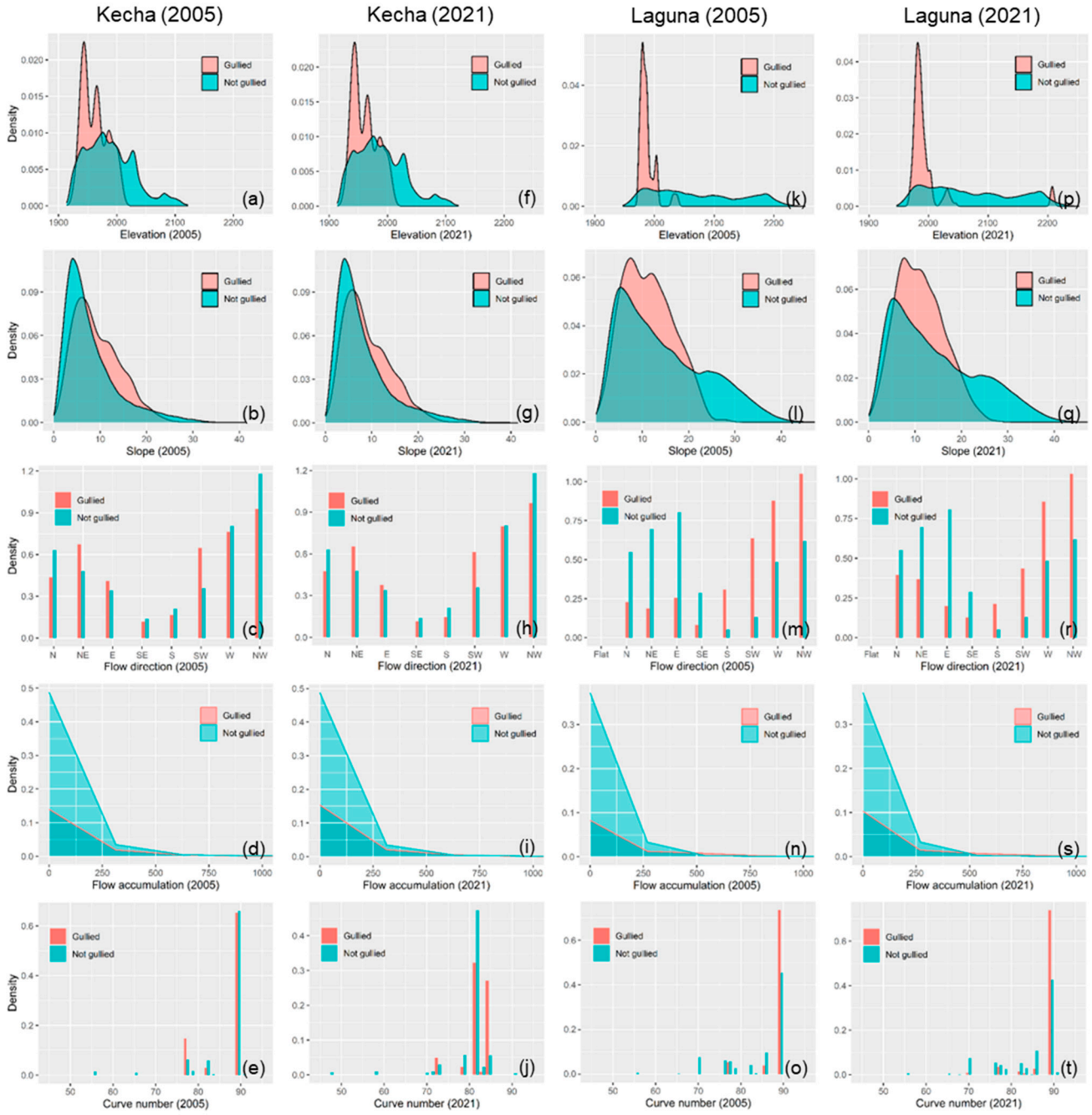


**Figure 5.** Density plots showing the response of geomorphic input variables for gullied and non-gullied areas in 2005 and 2021 for Kecha (left panel) and Laguna (right panel) watersheds: (**a**,**f**,**k**,**p**) elevation, (**b**,**g**,**l**,**q**) slope, (**c**,**h**,**m**,**r**) flow direction, (**d**,**i**,**n**,**s**) flow accumulation, and (**e**,**j**,**o**,**t**) curve number maps. NE: north-east; N: north; NW: north-west; W: west; SW: south-west; S: south; SE: south-east; E: east.

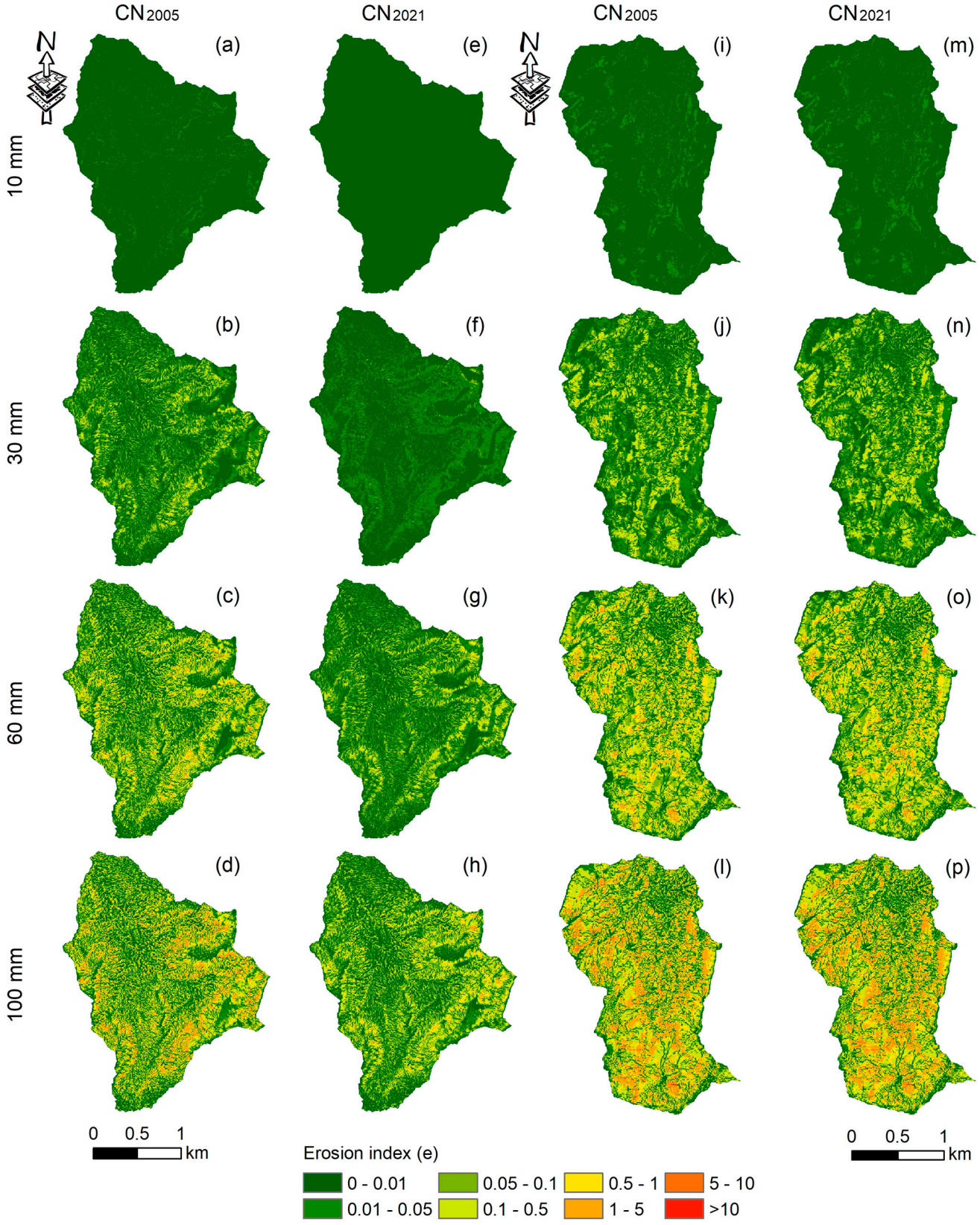


**Figure 6.** LANDPLANER-simulated erosion indices: for (**a**,**i**) $CN_{2005}$ and 10 mm, (**b**,**j**) $CN_{2005}$ and 30 mm, (**c**,**k**) $CN_{2005}$ and 60 mm, (**d**,**l**) $CN_{2005}$ and 100 mm, (**e**,**m**) $CN_{2021}$ and 10 mm, (**f**,**n**) $CN_{2021}$ and 30 mm, (**g**,**o**) $CN_{2021}$ and 60 mm, and (**h**,**p**) $CN_{2021}$ and 100 mm scenarios in Kecha (left panel) and Laguna (right panel) watersheds.

In addition, the prediction capabilities of the erosion indices exceeding certain critical thresholds (i.e., 0.01, 0.05, 0.1, 0.5, 1, 5, and 10) were tested for all curve number and rainfall scenarios. The performance of erosion indices exceeding these critical thresholds varied between 0 and 1 (reported using the TPR, TNR, FPR, FNR, and OA metrics) and was summarized in confusion matrices (Tables S6 and S7). Despite the predicted results showing higher OA (close to 1) for the majority of rainfall, curve number, and erosion index threshold combinations, most of them did not achieve good values of both TPR and TNR (i.e., >0.5) at the same time.

The overall analysis of the predicted results showed that the TNR performances increased as the erosion index thresholds increased but at the expense of decreasing TPR. As can be seen in Table 2, the best performances for gully channel-based predictions were obtained for a rainfall amount of 100 mm in Kecha (using $e > 0.1$ in $CN_{2005}$) and for a rainfall amount of 60 mm in Laguna (using $e > 0.1$ in $CN_{2005}$). Similarly, the best performances for gully head-based predictions were achieved for a 100 mm rainfall in Kecha (using $e > 0.1$ in $CN_{2021}$) and for a rainfall amount of 60 mm in Laguna (using $e > 0.1$ in $CN_{2005}$). In either case, the gully head-based predictions performed better than most gully channel-based predictions. On the contrary, the worst performing scenario for all was found considering a rainfall amount of 10 mm (Tables S6 and S7). The predictions made by the best-performing erosion indices showed that Laguna achieved a slightly better performance than Kecha (Table 2; Figure 7). The fact that the 10 mm rainfall scenario showed lower performance in predicting gullies does not mean the model is bad; rather, it means the scenario showed the least correlation and hence cannot be used to predict gullies in the study area.

**Table 2.** A confusion matrix table showing the prediction performance of different erosion index ($e$) thresholds for rainfall amounts of 100 mm for Kecha and 60 mm for Laguna watersheds.

| Watershed | Scenario | | $e$ | Gully Channel-Based Performance | | | | | | Gully Head-Based Performance | | | | | |
|---|---|---|---|---|---|---|---|---|---|---|---|---|---|---|---|
| | Curve Number | Rainfall (mm) | | TPR | TNR | FPR | FNR | OA | $\frac{TPR+TNR}{2}$ | TPR | TNR | FPR | FNR | OA | $\frac{TPR+TNR}{2}$ |
| Kecha | $CN_{2005}$ (untreated) | 100 | 0.01 | 0.557 | 0.400 | 0.600 | 0.443 | 0.401 | 0.478 | 0.848 | 0.400 | 0.600 | 0.152 | 0.400 | 0.624 |
| | | | 0.05 | 0.557 | 0.400 | 0.600 | 0.443 | 0.402 | 0.478 | 0.848 | 0.401 | 0.599 | 0.152 | 0.401 | 0.625 |
| | | | 0.1 | 0.495 | 0.494 | 0.506 | 0.505 | 0.494 | 0.495 | 0.758 | 0.494 | 0.506 | 0.242 | 0.494 | 0.626 |
| | | | 0.5 | 0.230 | 0.799 | 0.201 | 0.770 | 0.794 | 0.515 | 0.394 | 0.799 | 0.201 | 0.606 | 0.799 | 0.597 |
| | | | 1 | 0.121 | 0.905 | 0.095 | 0.879 | 0.898 | 0.513 | 0.242 | 0.905 | 0.095 | 0.758 | 0.905 | 0.574 |
| | | | 5 | 0.012 | 0.997 | 0.003 | 0.988 | 0.988 | 0.505 | 0.030 | 0.997 | 0.003 | 0.970 | 0.997 | 0.514 |
| | | | 10 | 0.002 | 1.000 | 0.000 | 0.998 | 0.991 | 0.501 | 0.000 | 1.000 | 0.000 | 1.000 | 0.999 | 0.500 |
| | $CN_{2021}$ (treated) | 100 | 0.01 | 0.552 | 0.400 | 0.600 | 0.448 | 0.401 | 0.476 | 0.750 | 0.400 | 0.600 | 0.250 | 0.401 | 0.575 |
| | | | 0.05 | 0.551 | 0.402 | 0.598 | 0.449 | 0.404 | 0.477 | 0.750 | 0.403 | 0.597 | 0.250 | 0.403 | 0.576 |
| | | | 0.1 | 0.386 | 0.670 | 0.330 | 0.614 | 0.667 | 0.528 | 0.525 | 0.669 | 0.331 | 0.475 | 0.669 | 0.597 |
| | | | 0.5 | 0.088 | 0.947 | 0.053 | 0.912 | 0.939 | 0.517 | 0.100 | 0.947 | 0.053 | 0.900 | 0.947 | 0.523 |
| | | | 1 | 0.030 | 0.988 | 0.012 | 0.970 | 0.979 | 0.509 | 0.050 | 0.988 | 0.012 | 0.950 | 0.988 | 0.519 |
| | | | 5 | 0.000 | 1.000 | 0.000 | 1.000 | 0.990 | 0.500 | 0.000 | 1.000 | 0.000 | 1.000 | 1.000 | 0.500 |
| | | | 10 | 0.000 | 1.000 | 0.000 | 1.000 | 0.990 | 0.500 | 0.000 | 1.000 | 0.000 | 1.000 | 1.000 | 0.500 |
| Laguna | $CN_{2005}$ (untreated) | 60 | 0.01 | 0.640 | 0.293 | 0.707 | 0.360 | 0.294 | 0.466 | 0.846 | 0.293 | 0.707 | 0.154 | 0.293 | 0.570 |
| | | | 0.05 | 0.640 | 0.296 | 0.704 | 0.360 | 0.297 | 0.468 | 0.846 | 0.296 | 0.704 | 0.154 | 0.296 | 0.571 |
| | | | 0.1 | 0.547 | 0.516 | 0.484 | 0.453 | 0.516 | 0.532 | 0.769 | 0.516 | 0.484 | 0.231 | 0.516 | 0.643 |
| | | | 0.5 | 0.203 | 0.852 | 0.148 | 0.797 | 0.850 | 0.528 | 0.231 | 0.852 | 0.148 | 0.769 | 0.852 | 0.542 |
| | | | 1 | 0.063 | 0.952 | 0.048 | 0.937 | 0.948 | 0.507 | 0.077 | 0.952 | 0.048 | 0.923 | 0.951 | 0.514 |
| | | | 5 | 0.004 | 0.999 | 0.001 | 0.996 | 0.995 | 0.501 | 0.000 | 0.999 | 0.001 | 1.000 | 0.999 | 0.499 |
| | | | 10 | 0.000 | 1.000 | 0.000 | 1.000 | 0.996 | 0.500 | 0.000 | 1.000 | 0.000 | 1.000 | 1.000 | 0.500 |
| | $CN_{2021}$ (untreated) | 60 | 0.01 | 0.621 | 0.293 | 0.707 | 0.379 | 0.295 | 0.457 | 0.760 | 0.293 | 0.707 | 0.240 | 0.293 | 0.527 |
| | | | 0.05 | 0.621 | 0.296 | 0.704 | 0.379 | 0.298 | 0.458 | 0.760 | 0.296 | 0.704 | 0.240 | 0.297 | 0.528 |
| | | | 0.1 | 0.526 | 0.508 | 0.492 | 0.474 | 0.508 | 0.517 | 0.560 | 0.508 | 0.492 | 0.440 | 0.508 | 0.534 |
| | | | 0.5 | 0.194 | 0.850 | 0.150 | 0.806 | 0.844 | 0.522 | 0.160 | 0.849 | 0.151 | 0.840 | 0.849 | 0.505 |
| | | | 1 | 0.071 | 0.952 | 0.048 | 0.929 | 0.945 | 0.511 | 0.080 | 0.951 | 0.049 | 0.920 | 0.951 | 0.516 |
| | | | 5 | 0.002 | 0.999 | 0.001 | 0.998 | 0.991 | 0.500 | 0.000 | 0.999 | 0.001 | 1.000 | 0.999 | 0.499 |
| | | | 10 | 0.000 | 1.000 | 0.000 | 1.000 | 0.992 | 0.500 | 0.000 | 1.000 | 0.000 | 1.000 | 1.000 | 0.500 |

$CN_{2005}$: curve number scenario in 2005; $CN_{2021}$: curve number scenario in 2021; $e$: erosion index; TPR: true positive rate; TNR: true negative rate; FPR: false positive rate; FNR: false negative rate; OA: overall accuracy. Note: values in bold red, yellow, and green indicate prediction performances between 0.4 and 0.45, between 0.45 and 0.5, and greater than or equal to 0.5, respectively, while the green, yellow, and orange highlighted rows show the best predictions in decreasing order achieved by a specific erosion index threshold.

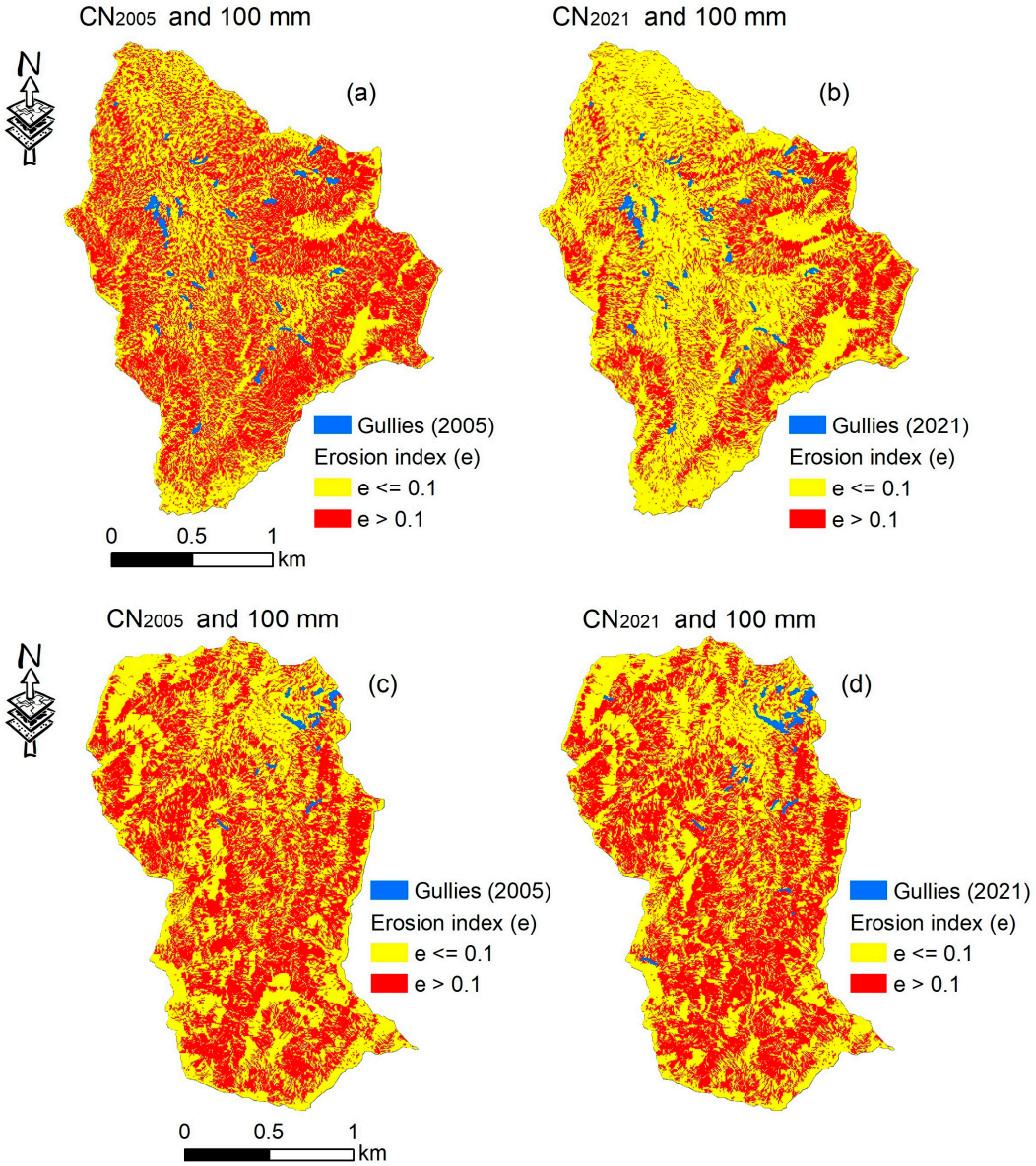


**Figure 7.** The best predictions made by LANDPLANER considering a simulated erosion index (*e*) exceeding a critical threshold of 0.1 in Kecha (top) and Laguna (bottom) for (**a**) $CN_{2005}$ and 100 mm, (**b**) $CN_{2021}$ and 100 mm, (**c**) $CN_{2005}$ and 60 mm, and (**d**) $CN_{2021}$ and 60 mm.

#### 4.2.2. Performance of Topographic (*esp*) and Erosion Channel (*esp_channel*) Thresholds for Different Curve Number Scenarios

The predicted *esp* and *esp_channel* maps (Figure 8) showed that more areas of Kecha watershed in $CN_{2005}$ were predicted as potentially gullied areas compared to the $CN_{2021}$ scenario. The corresponding accuracy assessment results (Table 3) also indicated that $CN_{2005}$ scenarios in both watersheds were better in predicting most gully heads and erosion channels than the $CN_{2021}$ scenario. In addition, although *esp* and *esp_channel* yielded comparable performances, the use of *erosion_channel* $\geq 1$ was found to slightly improve the performance of most gully erosion predictions compared to *esp*. Similar to the dynamic indices, gully head-based predictions showed better performances than gully channel-based predictions for most of the static thresholds, with Laguna scoring a higher performance than Kecha (Table 3).

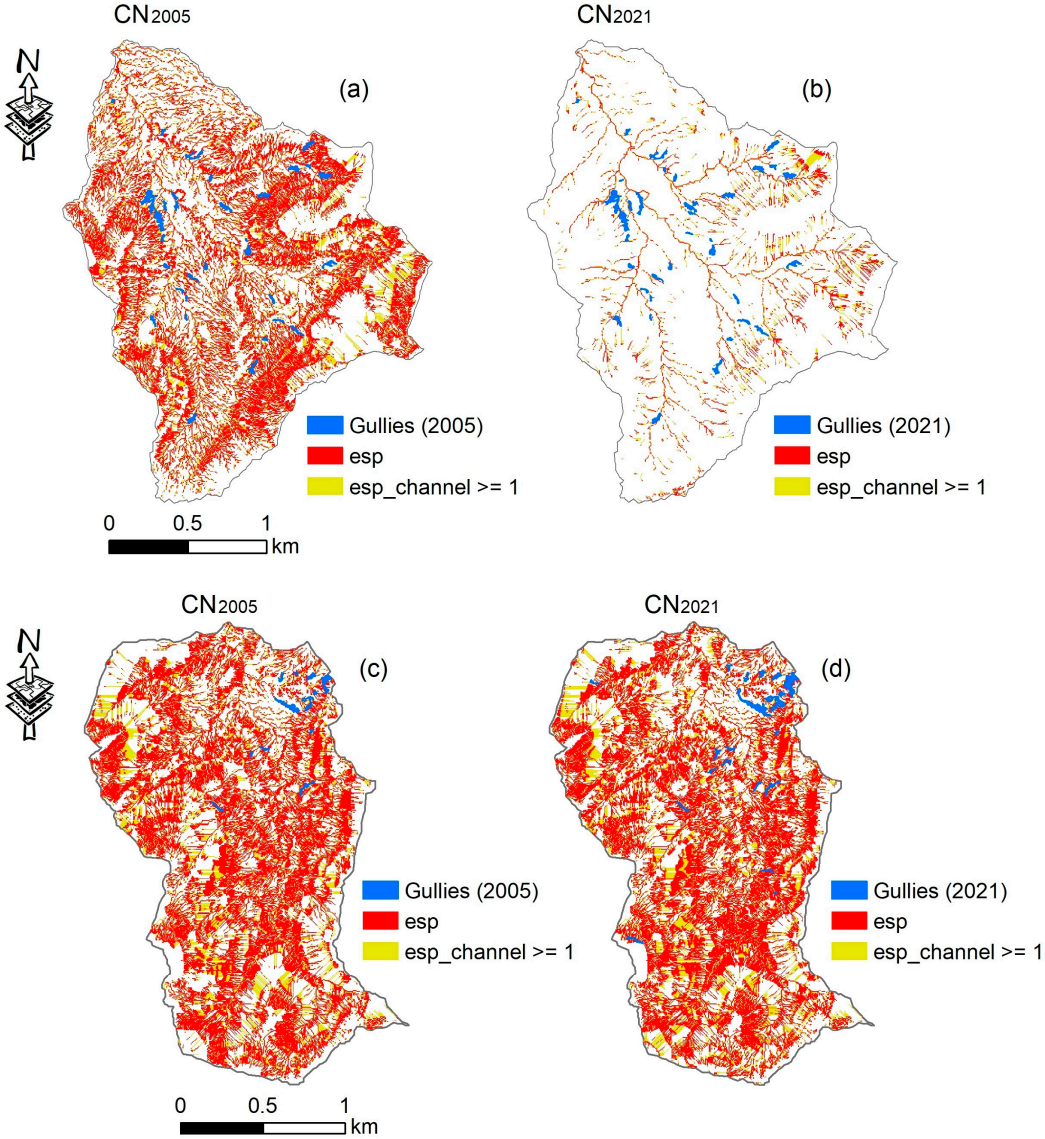


**Figure 8.** LANDPLANER-simulated results of the topographic threshold (*esp*) and erosion channel (*esp_channel*) exceeding a critical threshold of 1 for (**a**) Kecha in 2005, (**b**) Kecha in 2021, (**c**) Laguna in 2005, and (**d**) Laguna in 2021.

**Table 3.** A confusion matrix table showing the prediction performances of topographic (*esp*) and erosion channel (*esp_channel*) thresholds.

| Watershed | Threshold | Scenario | Gully Channel-Based Performance | | | | | | Gully Head-Based Performance | | | | | |
|---|---|---|---|---|---|---|---|---|---|---|---|---|---|---|
| | | Curve Number | TPR | TNR | FPR | FNR | OA | $\frac{TPR+TNR}{2}$ | TPR | TNR | FPR | FNR | OA | $\frac{TPR+TNR}{2}$ |
| Kecha (treated) | *esp* | $CN_{2005}$ | 0.411 | 0.666 | 0.334 | 0.589 | 0.664 | 0.539 | 0.515 | 0.666 | 0.334 | 0.485 | 0.666 | 0.590 |
| | | $CN_{2021}$ | 0.083 | 0.951 | 0.049 | 0.917 | 0.942 | 0.517 | 0.150 | 0.951 | 0.049 | 0.850 | 0.950 | 0.550 |
| | *esp_channel* | $CN_{2005}$ | 0.540 | 0.545 | 0.455 | 0.460 | 0.545 | 0.543 | 0.667 | 0.544 | 0.456 | 0.333 | 0.544 | 0.606 |
| | | $CN_{2021}$ | 0.145 | 0.913 | 0.087 | 0.855 | 0.906 | 0.529 | 0.250 | 0.913 | 0.087 | 0.750 | 0.913 | 0.581 |
| Laguna (untreated) | *esp* | $CN_{2005}$ | 0.619 | 0.578 | 0.422 | 0.381 | 0.578 | 0.599 | 0.692 | 0.577 | 0.423 | 0.308 | 0.577 | 0.635 |
| | | $CN_{2021}$ | 0.587 | 0.575 | 0.425 | 0.413 | 0.575 | 0.581 | 0.680 | 0.574 | 0.426 | 0.320 | 0.574 | 0.627 |
| | *esp_channel* | $CN_{2005}$ | 0.760 | 0.443 | 0.557 | 0.240 | 0.444 | 0.601 | 0.846 | 0.442 | 0.558 | 0.154 | 0.442 | 0.644 |
| | | $CN_{2021}$ | 0.698 | 0.430 | 0.570 | 0.302 | 0.432 | 0.564 | 0.760 | 0.429 | 0.571 | 0.240 | 0.429 | 0.595 |

*esp*: topographic threshold; *esp_channel*: erosion channel; $CN_{2005}$: curve number scenario in 2005; $CN_{2021}$: curve number scenario in 2021; TPR: true positive rate; TNR: true negative rate; FPR: false positive rate; FNR: false negative rate; OA: overall accuracy. Note: Values in bold red, yellow, and green colors indicate prediction performances below 0.4, between 0.4 and 0.5, and greater than or equal to 0.5, respectively, while the green, yellow, and red highlighted rows show the best predictions in decreasing order achieved by a specific erosion index threshold.

### *4.3. Impact of Rainfall Variability, LULC Changes, and LUM Practices on Gully Erosion in the Paired Watersheds*

The results showed that, despite the average erosion-triggering potential of a 10 mm rainfall being insignificant for both watersheds across all curve number scenarios, it increased to 0.03, 0.15, and 0.35 for Kecha in 2005; 0.01, 0.04, and 0.12 for Kecha in 2021; 0.05, 0.25, and 0.66 for Laguna in 2005; and 0.05, 0.25, and 0.67 for Laguna in 2021 for 30, 60, and 100 mm of rainfall, respectively (Table 4). The erosion triggering potential of the 60 and 100 mm rainfall scenarios in Kecha were 4–5 and 10–17 times higher than the 30 mm rainfall scenario, respectively. Similarly, the 60 mm and 100 mm rainfall scenarios in Laguna were 5 and 13 times higher than the 30 mm rainfall scenario, respectively. These results indicated that the impact of rainfall for Kecha was 64–79% lower in 2021 compared to the same thresholds in 2005, whereas Laguna showed little change (i.e., only 0–2% higher) between 2005 and 2021 (Table 4). The percentage change of topographic thresholds (*esp*) in Kecha showed a reduction of gully initiation areas by 28% (from 33% in 2005 to 5% in 2021). On the contrary, Laguna showed a little increment of gully initiation areas by only 1% (from 42% to 43%) during the same period (Table 4).

**Table 4.** The impact of rainfall and past and present curve number scenarios on gully initiation in Kecha and Laguna watersheds.

| Watershed | Scenario | | Impact of Rainfall | | | | | | Gully Initiation | | |
|---|---|---|---|---|---|---|---|---|---|---|---|
| | Curve Number | Rainfall (mm Day$^{-1}$) | Min. | Max. | Mean | St. Dev. | Times * (Compared to 30 mm) | Change ** (%) (from 2005) | Gully Initiation (Pixels) | Gully Initiation (%) | Change ** (%) (from 2005) |
| Kecha | $CN_{2005}$ | 10 | 0.00 | 0.05 | 0.00 | 0.00 | - | - | 53,585 | 33 | - |
| | | 30 | 0.00 | 1.37 | 0.03 | 0.06 | - | - | | | |
| | | 60 | 0.00 | 8.78 | 0.15 | 0.29 | 4 | - | | | |
| | | 100 | 0.00 | 28.45 | 0.35 | 0.72 | 10 | - | | | |
| | $CN_{2021}$ | 10 | 0.00 | 0.01 | 0.00 | 0.00 | - | - | 7910 | 5 | −28 |
| | | 30 | 0.00 | 0.24 | 0.01 | 0.01 | - | −79 | | | |
| | | 60 | 0.00 | 2.36 | 0.04 | 0.07 | 5 | −72 | | | |
| | | 100 | 0.00 | 12.57 | 0.12 | 0.25 | 17 | −64 | | | |
| Laguna | $CN_{2005}$ | 10 | 0.00 | 0.06 | 0.00 | 0.00 | - | - | 58,145 | 42 | - |
| | | 30 | 0.00 | 2.29 | 0.05 | 0.08 | - | - | | | |
| | | 60 | 0.00 | 17.44 | 0.25 | 0.47 | 5 | - | | | |
| | | 100 | 0.00 | 48.73 | 0.66 | 1.32 | 13 | - | | | |
| | $CN_{2021}$ | 10 | 0.00 | 0.06 | 0.00 | 0.00 | - | - | 58,633 | 43 | 1 |
| | | 30 | 0.00 | 2.25 | 0.05 | 0.08 | - | 0 | | | |
| | | 60 | 0.00 | 13.03 | 0.25 | 0.46 | 5 | 1 | | | |
| | | 100 | 0.00 | 53.82 | 0.67 | 1.31 | 13 | 2 | | | |

CN2005: Curve number scenario in 2005; CN2021: Curve number scenario in 2021; Min.: minimum; Max.: maximum; St. Dev.: standard deviation. * The mean erosive potentials of the 60 and 100 mm rainfalls were equal to the reported results times the mean erosive power of the 30 mm rainfall. ** The mean change in the erosive potentials of the 30, 60 and 100 mm rainfalls for the $CN_{2021}$ scenario compared to the same rainfall amounts in $CN_{2005}$.

The comparison of different alternative land use planning options in Laguna (Figure 9; Table S8) also showed that the impact of rainfall on gully initiation could be reduced by 3–6% for $CN_{option1}$ due to LULC conversion, by 94–96% for $CN_{option2}$ due to LUM options, and by 89–93% for $CN_{option3}$ due to changes in LULC and LUM options (Table 5). As a result, the separate impact of LULC conversion could reduce gully initiation by only 1%, while the separate implementation of LUM options significantly reduced gully initiation by 39%. In addition, gully initiation was reduced by 37% when LULC and LUM options were combined (Table 5).

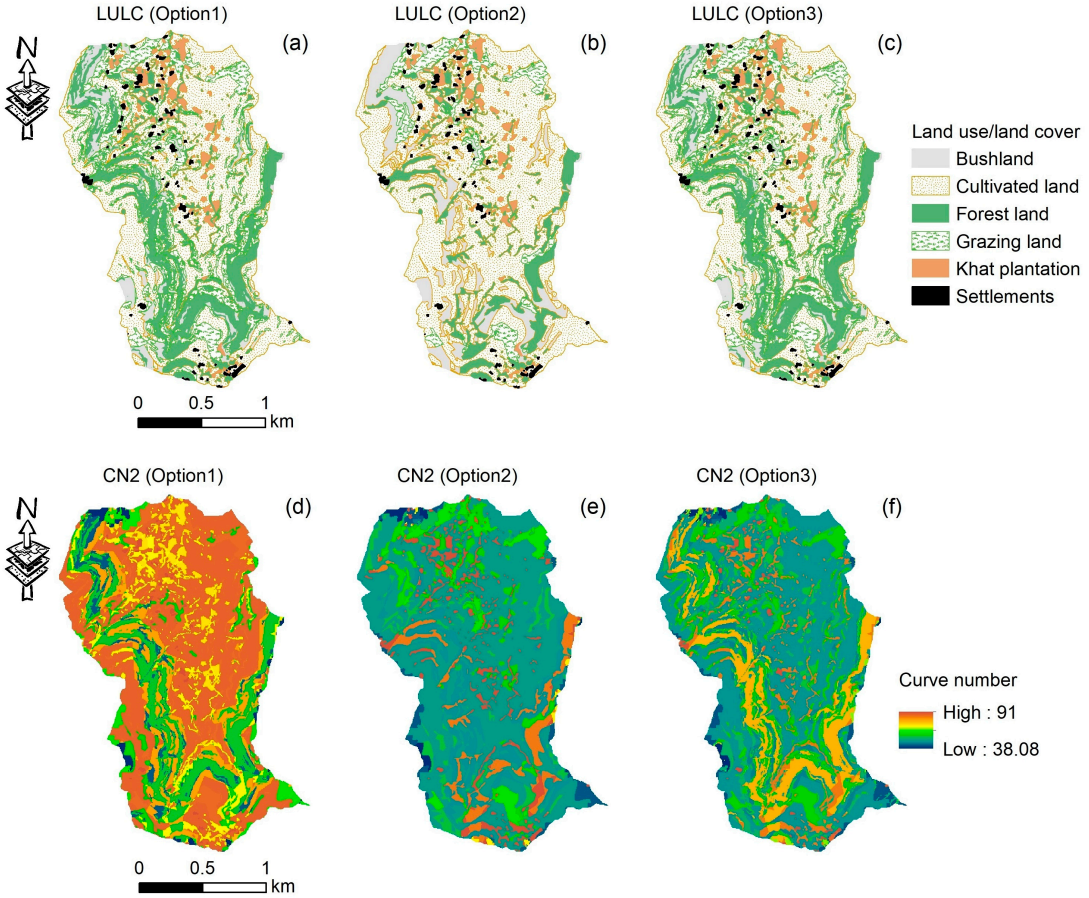


**Figure 9.** The land use/land cover (LULC) and curve number (CN2) maps of the proposed alternative land use planning options in the Laguna watershed: (**a**) LULC for Option1, (**b**) LULC for Option2, (**c**) LULC for Option3, (**d**) CN2 for Option1, (**e**) CN2 for Option2, and (**f**) CN2 for Option3. See Tables S4 and S8 for the derivation of the runoff curve number-II.

**Table 5.** The impact of different rainfall and alternative land use planning options on gully initiation in the Laguna watershed.

| Watershed | Scenario | | Impact of Rainfall | | | | | | Gully Initiation | | |
|---|---|---|---|---|---|---|---|---|---|---|---|
| | Curve Number | Rainfall (mm Day$^{-1}$) | Min. | Max. | Mean | St. Dev. | Times * (Compared to 30 mm) | Change ** (%) (from Baseline) | Gully Initiation (Pixels) | Gully Initiation (%) | Change ** (%) (from Baseline) |
| Laguna | $CN_{2021}$ (Baseline) | 10 | 0.00 | 0.06 | 0.00 | 0.00 | - | - | 58,633 | 43 | - |
| | | 30 | 0.00 | 2.25 | 0.05 | 0.08 | - | - | | | |
| | | 60 | 0.00 | 13.03 | 0.25 | 0.46 | 5 | - | | | |
| | | 100 | 0.00 | 53.82 | 0.67 | 1.31 | 13 | - | | | |
| | $CN_{option1}$ | 10 | 0.00 | 0.06 | 0.00 | 0.00 | - | - | 57,838 | 42 | −1 |
| | | 30 | 0.00 | 2.02 | 0.05 | 0.08 | - | −6 | | | |
| | | 60 | 0.00 | 12.10 | 0.24 | 0.43 | 5 | −5 | | | |
| | | 100 | 0.00 | 46.27 | 0.65 | 1.23 | 13 | −3 | | | |
| | $CN_{option2}$ | 10 | 0.00 | 0.04 | 0.00 | 0.00 | - | - | 4971 | 4 | −39 |
| | | 30 | 0.00 | 0.52 | 0.00 | 0.01 | - | −96 | | | |
| | | 60 | 0.00 | 1.86 | 0.01 | 0.05 | 5 | −95 | | | |
| | | 100 | 0.00 | 6.14 | 0.04 | 0.16 | 17 | −94 | | | |
| | $CN_{option3}$ | 10 | 0.00 | 0.04 | 0.00 | 0.00 | - | - | 8144 | 6 | −37 |
| | | 30 | 0.00 | 0.53 | 0.00 | 0.01 | - | −93 | | | |
| | | 60 | 0.00 | 1.89 | 0.02 | 0.06 | 5 | −91 | | | |
| | | 100 | 0.00 | 8.04 | 0.07 | 0.21 | 18 | −89 | | | |

CN2005: Curve number scenario in 2005; CN2021: Curve number scenario in 2021; Min.: minimum; Max.: maximum; St. Dev.: standard deviation. * The mean erosive potentials of the 60 and 100 mm rainfalls were equal to the reported results times the mean erosive power of the 30 mm rainfall. ** The mean change in the erosive potentials of the 30, 60 and 100 mm rainfalls for the $CN_{2021}$ scenario compared to the same rainfall amounts in $CN_{2005}$.

## 5. Discussion

Studies showed that the initiation and expansion of gullies could be affected by LULC and climate in addition to the topographic and soil-related factors [1,6,8]. This study investigated the effect of changes in rainfall, LULC, and LUM practices on the spatio-temporal modeling of gully erosion using geomorphic and curve number maps as an input for the distributed LANDPLANER model [23,24].

Before applying LANDPLANER, the density plots of input factors explained that gullies were mostly found in low-lying areas with relatively higher curve number values in NW-facing gentle slopes (Figure 5). The higher curve number value of gullies indicated that gullies might be initiated by the surface runoff generated in the study watersheds (see Equations (1) and (2); [24]). The relatively higher curve number for gullies in the untreated Laguna watershed was due to the lack of existing LUM practices in the watershed compared to the treated Kecha watershed [33]. In agreement with this, recent studies reported that most gullies in the study watersheds were concentrated in low-lying, higher curve number, and gentle slope (less than 15°) areas compared to hillslope areas with steep slopes, where lower flow accumulation is expected [16,17]. This is mainly because gullies are threshold-dependent phenomena, and their initiation is expressed by an inverse power relationship of slope and contributing area [25,27,48]. Since a subsurface flow is not common at Aba Gerima, the initiation of gullies in low-lying areas is more likely caused by an overland flow due to the absence of subsurface flow and the predominance of Hortonian overland flow for the development of gullies in the study area. For gentle slopes in low-lying elevation areas, the surface runoff at a point increase with increasing curve number and upslope contributing area that could eventually exceed the critical topographic threshold and trigger the initiation or continue the expansion of the gully at that point [25,26]. Despite the classical topographic threshold approach does not explicitly account for the effect of curve number, Equation (5) an equation proposed by Torri and Poesen [25] accounts its effect as can be seen from Equation (5). With this regard, the use of LANDPLANER was found advantageous for directly considering the curve number from $S_{0.05}$ (see Equation (2)) to predict topographic thresholds. The drainage directions in the study areas showed a relatively wider distribution with certain preferences towards the NW direction (Figure 5) along drainage networks. This means many gullies found on the right side of the watersheds facing NW are close to streamlines. Geroy et al. [49] reported that differences in the depth and grain size of soil materials could affect the water retention capacity of soils in specific slope aspects/flow directions. In addition to watershed geometry, the drainage direction may also influence the spatial distribution of soil moisture, vegetation density, and erosion processes of the watershed [9], which create favorable conditions for gullies to initiate and expand. Similar studies using topographic, statistical, and machine-learning approaches have reported that flow direction could strongly influence the presence of gullies [50–54].

The LANDPLANER-simulated dynamic and static thresholds were also used to evaluate the effect of changes in rainfall and curve number scenarios on modeling the spatial and temporal distribution of gully erosion (Tables 2 and 3). The variation of the dynamic $e$ for changes in rainfall scenarios was significant compared to changes in the curve number scenarios considered (see Figure 6). The main reason for this may be because of small changes in the LULC in the study watersheds between the past and present scenarios (Table S2). However, rainfall variation could also have the main influence on the initiation and development of gullies in the study area compared to LULC. A study conducted in a small watershed in the Mediterranean environment of Spain reported that, despite the effect of LULC could be higher during low rainfall periods, rainfall has the primary control over the initiation of gully heads during higher rainfall periods, with LULC exerting only a secondary control [11]. Vanmaercke et al. [5] also reported that the rainy day normal significantly correlated to gully headcut retreat rates. These results confirm the fact that gully heads are mostly formed in areas with higher curve numbers and are triggered by higher rainfall magnitudes [9]. The analysis of the predicted results showed that the performance

of the model measured by TNR increased with values of the *e* threshold, decreasing the TPR metrics and suggesting that more areas were wrongly predicted as gully by smaller *e* thresholds than larger ones. The predictive performance evaluation of various *e* thresholds showed that the worst performance was obtained for a rainfall amount of 10 mm, which showed the least correlation with the occurrence of gullies which indicated that the same amount of rainfall might not be enough to initiate or expand gullies in the study area. Studies reported that a minimum daily rainfall depth of 15–18 mm is required to initiate (ephemeral) gullies in croplands with silt loamy soils [1,18,46]. On the contrary, the best model predictions achieved considering $e > 0.1$ for a 100 mm rainfall in Kecha and a 60 mm rainfall in Laguna (Table 2) suggest that the prediction of gullies in the study area is highly variable depending on watershed characteristics. Hence, the best model prediction for gullies in other study areas needs to consider the morphological, climatic, LULC, and LUM conditions of the areas instead of extrapolation. The higher rainfall amount in Kecha likely reflects the higher resistance of the soil [25,26] for smaller rainfall magnitudes due to better LULC and LUM practices in the watershed [33]. In fact, most areas in Kecha have relatively lower curve number values (higher infiltration rate) due to protected grazing and bushlands and better coverage of LUM practices. The result that showed gully head-based predictions were slightly better than gully channel-based predictions (Table 2) is in agreement with other studies [9,10] that employed LANDPLANER. This is attributed to the fact that the performance assessment of gully channel-based assessments considers not only gully head pixels but also other pixels within the gully boundary, which gives rise to prediction errors. Agostini et al. [10] associated the lower accuracy predictions with the fulfillment and quality of the gully inventory maps used. In addition, other processes may play the role for gully channels. Overall, the results indicated that $e > 0.1$ could be used to predict gully erosion from a slightly higher to good accuracy compared to a simple random prediction with TPR and TNR values of 0.5. Similarly, the static *esp* and *esp_channel* thresholds were used to predict gully initiation and the resulting erosion channel for the past and present LULC and LUM scenarios (Figure 8). The analysis of the static results showed that both *esp* and *esp_channel* thresholds for the past ($CN_{2005}$) scenario predicted gully initiation and erosion channels better than the present ($CN_{2021}$) scenario, showing slightly higher correlation (Table 3).The use of *esp_channel* showed better overall predictive capability than that of *esp* for most predictions. This is because *esp_channel* better resembles gully polygons, as they incorporate additional downslope areas other than erosion starting *esp* points that represent gully heads [23]. Although the predicted results of *esp* and *esp_channel* showed good average maximized performances of TPR and TNR, some of their TPR and TNR performances were worse than an average random estimation (Table 3). This could be attributed to one or more of the following factors: (1) uncertainties in the source and resolutions of datasets used; (2) differences in the stages of gully development; (3) bias to unaccounted factors in the slope–area relationships. First, there might be uncertainties related to the acquisition and analysis of different sources of remote sensing datasets (i.e., satellite images and DEM maps) that cannot be fully resolved even with the aid of field surveys [10]. For instance, a machine learning-based gully erosion susceptibility assessment carried out in the study watersheds showed that the spatial resolution of DEM-derived factors could affect the prediction performance of the model [17]. Second, differences in the geomorphological stages of gullies need to be accounted. Sidorchuk [55] modeled gully erosion separately by considering two different stages of gully development as a dynamic and static stage, representing the initial and final geomorphological stages of gully development, respectively. Hence, the older gullies might be presently considered as streams when the geomorphologically dynamic gully systems that developed in the past evolved to be part of well-defined and stabilized stream networks. The static threshold maps intersected with most of the river networks in the study watersheds (Figure 8), as gullies also depend on the size of contributing areas like streams [25,27,48]. Third, bias in the unaccounted factors in slope–area relationships (such as land use and management, rainfall, and topographic characteristics) might have impacted the predictive performance

of the static thresholds of the model. Rossi et al. [24] reported that the land use considered may not truly represent the situation of gullies at the time of gully initiation and development since gullies might be older than the land use mapped later. When studying gullies, the LULC to be considered should be at the moment of gully development [26]. Another potential reason could be the difference between the actual and topographically derived contributing areas at gully heads. This happens when the duration of rainfall (with specific intensity-duration-frequency characteristics) is less than the minimum time of concentration required to hydrologically connect the whole contributing areas at the gully heads [24]. Similarly, the recent land management activities may also have an impact on altering the contributing areas of gully heads, which is an important parameter for the static thresholds of the model [56]. The *fanya juu* terraces, soil, and stone bunds are common land management practices in Kecha in addition to the traditional field plot boundaries and drainage ditches [33].

The erosive impact of rainfall in the untreated Laguna watershed slightly increased (by only 0–2%) between 2005 and 2021 due to LULC, while it significantly reduced in the treated Kecha watershed (by 64–79%) during the same period due to LULC and LUM. Similarly, the gully initiation area in Laguna showed little increment (by only 1%) due to LULC, while it significantly reduced (by 28%) due to LULC and LUM. Furthermore, gully initiation areas for the future predicted that alternative land use planning options in Laguna could be reduced by 1% due to LULC options, 39% due to LUM options, and 37% due to LULC and LUM options. The gully initiation increased from $CN_{option2}$ to $CN_{option3}$ since there are more converted forests in $CN_{option3}$ that will not be treated by the proposed LUM alternatives (Figure 9). The results are in agreement with other studies conducted in the current study area [30,33] to study the impact of alternative land use planning options on runoff and sediment loss. Berihun et al. [33] reported that the implementation of LUM practices in Kecha reduced sediment yield in 2016 by 43% compared to its previous untreated condition in 2005 and by 51–68% compared to Laguna, while the combination of changes in LULC, LUM, and rainfall reduced sediment yield by 65–78%. In addition, Berihun et al. [30] reported that the proposed alternative land use planning options in Laguna could reduce sediment loss by 32–83% due to LULC options, 40–89% due to LUM options, and 95% when LULC and LUM options combined. These results showed that LUM practices outweigh the impact of LULC on gully initiation for the past, present, and future scenarios. Other studies conducted in different parts of Ethiopia also confirmed that different soil and water conservation practices were effective in reducing runoff and (gully) erosion (e.g., [57–59]).

Overall, the analysis of the dynamic and static threshold results for the past and present curve number conditions across various rainfall scenarios showed that LANDPLANER was capable of predicting the location of gullies in the study watersheds at a reasonable accuracy (with TPR = 0.667 and TNR = 0.544 for Kecha and TPR = 0.769 and TNR = 0.516 for Laguna). Despite slightly less than average random prediction performances observed in some cases, this study proved that the model can serve as an important tool to study the hydro-geomorphological processes of watersheds in general and gully erosion in particular. The model is even more advantageous for its relatively simple and quick predictions of gully occurrence with fewer data requirements compared to more complex and parameter-intensive process-based models and with less programming skill compared to most machine learning algorithms. Such qualities make the model preferable to predict gully erosion for data scare regions, where obtaining many input factors is difficult.

## 6. Conclusions and Recommendations

This study evaluated the effect of changes in rainfall, LULC, and LUM practices on the spatial and temporal modeling of gully erosion at (treated) Kecha and (untreated) Laguna watersheds in the Upper Blue Nile basin of Ethiopia using a distributed LANDPLANER model. Gullies in the study watersheds were mostly found in low-lying areas with higher curve number values and NW-facing gentle slopes. The performance of predicted results

showed that the dynamic index and static thresholds predicted gully erosion reasonably well. While the 10 mm rainfall had minimal erosion triggering potential, the 30, 60 and 100 mm rainfall scenarios had higher potential with increasing order. The impact of rainfall and the coverage of gully initiation areas between 2005 and 2021 was significantly reduced in the treated (Kecha) watershed due to LUM practices and insignificantly increased in the untreated (Laguna) watershed due to LULC changes. The analysis of the past, present, and future scenarios indicated that the LUM practices have a pronounced impact on reducing gully initiation in the study watersheds compared to LULC changes.

The main findings of this study clearly indicated that (1) changes in the rainfall and LUM practices significantly impacted gully initiation, and (2) LUM practices outweighed the impact of LULC on gully erosion in the study watersheds. Hence, future research and gully management activities should pay attention to rainfall magnitudes and LUM practices in addition to LULC.

The results imply that LANDPLANER can be used to study hydro-geomorphological processes and predict gully erosion, with some improvements needed to expand its applicability in the future. The model can further be improved by incorporating: (i) calibration tools that convert the erosion index to actual erosion rates and (ii) simulation techniques that directly consider the impact of single and multiple time series rainfall events on the model outputs, especially on static thresholds of the model.

**Supplementary Materials:** The following supporting information can be downloaded at: https://www.mdpi.com/article/10.3390/land12050947/s1.

**Author Contributions:** Conceptualization, T.A.S., A.T., N.H., M.T. and M.R.; data curation, T.A.S. and M.L.B.; formal analysis, T.A.S., M.R. and F.A.; funding acquisition, A.T., N.H. and M.T.; investigation, T.A.S., A.T., N.H., M.T., M.R. and F.A.; methodology, T.A.S., A.T., N.H., M.T., M.R. and F.A.; project administration, A.T., N.H. and M.T.; resources, T.A.S., A.T., N.H. and M.T.; software, T.A.S. and M.R.; supervision, A.T., N.H., M.T. and M.R.; validation, T.A.S.; visualization, T.A.S. and M.R.; writing—original draft, T.A.S.; writing—review and editing, T.A.S., A.T., N.H., M.T., M.R., F.A., M.V., S.D.G., A.A.F., K.E., M.Y., M.L.B., D.S., B.N. and T.M.M. All authors have read and agreed to the published version of the manuscript.

**Funding:** This research was funded by the Japan Society for the Promotion of Science (JSPS) bilateral project "Developing a gully erosion model for better land management" (grant number JPJSBP120212201) and the Science and Technology Research Partnership for Sustainable Development (SATREPS, grant number JPMJSA1601) project from the Japan Science and Technology Agency (JST)/Japan International Cooperation Agency (JICA).

**Data Availability Statement:** The data presented in this study are available upon request from the corresponding author.

**Acknowledgments:** The first author appreciates the financial supports received from the Japanese Government (MEXT) scholarship program and the International Platform for Dryland Research and Education (IPDRE) Sponsorship Program for Fostering Young Scientists. The authors thank the Arid Land Research Center at Tottori University for providing a suitable research environment.

**Conflicts of Interest:** The authors declare no conflict of interest.

## References

1. Poesen, J.; Nachtergaele, J.; Verstraeten, G.; Valentin, C. Gully erosion and environmental change: Importance and research needs. *Catena* **2003**, *50*, 91–133. [CrossRef]
2. Imeson, A.; Kwaad, F. Gully types and gully prediction. *Geogr. Tijdschr.* **1980**, *14*, 430–441.
3. Brice, J.C. *Erosion and Deposition in the Loess-Mantled Great Plains, Medicine Creek Drainage Basin, Nebraska*; US Government Printing Office: Washington, DC, USA, 1966.
4. Hauge, C. *Soil Erosion Definitions*; California Department of Forestry: Sacramento, CA, USA, 1977.
5. Vanmaercke, M.; Poesen, J.; Van Mele, B.; Demuzere, M.; Bruynseels, A.; Golosov, V.; Bezerra, J.F.R.; Bolysov, S.; Dvinskih, A.; Frankl, A.; et al. How fast do gully headcuts retreat? *Earth-Sci. Rev.* **2016**, *154*, 336–355. [CrossRef]
6. Vanmaercke, M.; Panagos, P.; Vanwalleghem, T.; Hayas, A.; Foerster, S.; Borrelli, P.; Rossi, M.; Torri, D.; Casali, J.; Borselli, L.; et al. Measuring, modelling and managing gully erosion at large scales: A state of the art. *Earth-Sci. Rev.* **2021**, *218*, 103637. [CrossRef]

7. Castillo, C.; Gómez, J. A century of gully erosion research: Urgency, complexity and study approaches. *Earth-Sci. Rev.* **2016**, *160*, 300–319. [CrossRef]
8. Valentin, C.; Poesen, J.; Li, Y. Gully erosion: Impacts, factors and control. *Catena* **2005**, *63*, 132–153. [CrossRef]
9. Kariminejad, N.; Rossi, M.; Hosseinalizadeh, M.; Pourghasemi, H.R.; Santosh, M. Gully head modelling in Iranian Loess Plateau under different scenarios. *Catena* **2020**, *194*, 104769. [CrossRef]
10. Agostini, M.; Mondini, A.C.; Torri, D.; Rossi, M. Modelling seasonal variation of gully erosion at the catchment scale. *Earth Surf. Process. Landf.* **2022**, *47*, 436–458. [CrossRef]
11. Hayas, A.; Poesen, J.; Vanwalleghem, T. Rainfall and vegetation effects on temporal variation of topographic thresholds for gully initiation in Mediterranean cropland and olive groves. *Land Degrad. Dev.* **2017**, *28*, 2540–2552. [CrossRef]
12. Amare, S.; Keesstra, S.; van der Ploeg, M.; Langendoen, E.; Steenhuis, T.; Tilahun, S. Causes and controlling factors of Valley bottom Gullies. *Land* **2019**, *8*, 141. [CrossRef]
13. Tebebu, T.; Abiy, A.; Zegeye, A.; Dahlke, H.; Easton, Z.; Tilahun, S.; Collick, A.; Kidnau, S.; Moges, S.; Dadgari, F.; et al. Surface and subsurface flow effect on permanent gully formation and upland erosion near Lake Tana in the northern highlands of Ethiopia. *Hydrol. Earth Syst. Sci.* **2010**, *14*, 2207–2217. [CrossRef]
14. Zegeye, A.D.; Langendoen, E.J.; Stoof, C.R.; Tilahun, S.A.; Dagnew, D.C.; Zimale, F.A.; Guzman, C.D.; Yitaferu, B.; Steenhuis, T.S. Morphological dynamics of gully systems in the subhumid Ethiopian Highlands: The Debre Mawi watershed. *Soil* **2016**, *2*, 443–458. [CrossRef]
15. Amare, S.; Langendoen, E.; Keesstra, S.; Ploeg, M.v.d.; Gelagay, H.; Lemma, H.; van der Zee, S.E. Susceptibility to gully erosion: Applying random forest (RF) and frequency ratio (FR) approaches to a small catchment in Ethiopia. *Water* **2021**, *13*, 216. [CrossRef]
16. Yibeltal, M.; Tsunekawa, A.; Haregeweyn, N.; Adgo, E.; Meshesha, D.T.; Aklog, D.; Masunaga, T.; Tsubo, M.; Billi, P.; Vanmaercke, M.; et al. Analysis of long-term gully dynamics in different agro-ecology settings. *Catena* **2019**, *179*, 160–174. [CrossRef]
17. Setargie, T.A.; Tsunekawa, A.; Haregeweyn, N.; Tsubo, M.; Fenta, A.A.; Berihun, M.L.; Sultan, D.; Yibeltal, M.; Ebabu, K.; Nzioki, B.; et al. Random Forest–based gully erosion susceptibility assessment across different agro-ecologies of the Upper Blue Nile basin, Ethiopia. *Geomorphology* **2023**, *431*, 108671. [CrossRef]
18. Poesen, J.; Torri, D.; Vanwalleghem, T. Gully erosion: Procedures to adopt when modelling soil erosion in landscapes affected by gullying. In *Handbook of Erosion Modelling*; Wiley Online Library: Hoboken, NJ, USA, 2011.
19. Hajigholizadeh, M.; Melesse, A.M.; Fuentes, H.R. Erosion and sediment transport modelling in shallow waters: A review on approaches, models and applications. *Int. J. Environ. Res. Public Health* **2018**, *15*, 518. [CrossRef]
20. Douglas-Mankin, K.R.; Roy, S.K.; Sheshukov, A.Y.; Biswas, A.; Gharabaghi, B.; Binns, A.; Rudra, R.; Shrestha, N.K.; Daggupati, P. A comprehensive review of ephemeral gully erosion models. *Catena* **2020**, *195*, 104901. [CrossRef]
21. Bzdok, D.; Altman, N.; Krzywinski, M. Statistics versus machine learning. *Nat Methods* **2018**, *15*, 233–234. [CrossRef]
22. Ferro, V.; Giordano, G.; Iovino, M. Isoerosivity and erosion risk map for Sicily. *Hydrol. Sci. J.* **1991**, *36*, 549–564. [CrossRef]
23. Rossi, M. Modeling of Landslide Phenomena and Erosion Processes Triggered by Meteo-Climatic Factors. Doctoral Dissertation, University of Perugia, Perugia, Italy, 2014. [CrossRef]
24. Rossi, M.; Torri, D.; Santi, E. Bias in topographic thresholds for gully heads. *Nat. Hazards* **2015**, *79*, 51–69. [CrossRef]
25. Torri, D.; Poesen, J. A review of topographic threshold conditions for gully head development in different environments. *Earth-Sci. Rev.* **2014**, *130*, 73–85. [CrossRef]
26. Torri, D.; Poesen, J.; Rossi, M.; Amici, V. Gully head modelling: A Mediterranean badland case study. *Earth Surf. Process. Landf.* **2018**, *43*, 2547–2561. [CrossRef]
27. Patton, P.C.; Schumm, S.A. Gully erosion, Northwestern Colorado: A threshold phenomenon. *Geology* **1975**, *3*, 88–90. [CrossRef]
28. Nyssen, J.; Clymans, W.; Descheemaeker, K.; Poesen, J.; Vandecasteele, I.; Vanmaercke, M.; Zenebe, A.; Van Camp, M.; Haile, M.; Haregeweyn, N.; et al. Impact of soil and water conservation measures on catchment hydrological response—A case in north Ethiopia. *Hydrol. Process.* **2010**, *24*, 1880–1895. [CrossRef]
29. Mhiret, D.A.; Dagnew, D.C.; Guzman, C.D.; Alemie, T.C.; Zegeye, A.D.; Tebebu, T.Y.; Langendoen, E.J.; Zaitchik, B.F.; Tilahun, S.A.; Steenhuis, T.S. A nine-year study on the benefits and risks of soil and water conservation practices in the humid highlands of Ethiopia: The Debre Mawi watershed. *J. Environ. Manag.* **2020**, *270*, 110885. [CrossRef]
30. Berihun, M.L.; Tsunekawa, A.; Haregeweyn, N.; Tsubo, M.; Fenta, A.A.; Ebabu, K.; Sultan, D.; Dile, Y.T. Reduced runoff and sediment loss under alternative land capability-based land use and management options in a sub-humid watershed of Ethiopia. *J. Hydrol. Reg. Stud.* **2022**, *40*, 100998. [CrossRef]
31. Ali, S.; Sethy, B.; Singh, R.; Parandiyal, A.; Kumar, A. Quantification of hydrologic response of staggered contour trenching for horti-pastoral land use system in small ravine watersheds: A paired watershed approach. *Land Degrad. Dev.* **2017**, *28*, 1237–1252. [CrossRef]
32. Melaku, N.D.; Renschler, C.S.; Holzmann, H.; Strohmeier, S.; Bayu, W.; Zucca, C.; Ziadat, F.; Klik, A. Prediction of soil and water conservation structure impacts on runoff and erosion processes using SWAT model in the northern Ethiopian highlands. *J. Soils Sediments* **2018**, *18*, 1743–1755. [CrossRef]
33. Berihun, M.L.; Tsunekawa, A.; Haregeweyn, N.; Dile, Y.T.; Tsubo, M.; Fenta, A.A.; Meshesha, D.T.; Ebabu, K.; Sultan, D.; Srinivasan, R. Evaluating runoff and sediment responses to soil and water conservation practices by employing alternative modeling approaches. *Sci. Total Environ.* **2020**, *747*, 141118. [CrossRef]

34. Wilson, G.; Shields, F.; Bingner, R.; Reid-Rhoades, P.; DiCarlo, D.; Dabney, S. Conservation practices and gully erosion contributions in the Topashaw Canal watershed. *J. Soil Water Conserv.* **2008**, *63*, 420–429. [CrossRef]
35. Anderson, R.L.; Rowntree, K.M.; Le Roux, J.J. An interrogation of research on the influence of rainfall on gully erosion. *Catena* **2021**, *206*, 105482. [CrossRef]
36. Hurni, H.; Berhe, W.; Chadhokar, P.; Daniel, D.; Gete, Z.; Grunder, M.; Kassaye, G. *Soil and Water Conservation in Ethiopia: Guidelines for Development Agents*; Centre for Development and Environment: Bern, Switzerland, 2016.
37. Mekonnen, G. *Soil Characterization, Classification and Mapping of Three Twin Watersheds in the Upper Blue Nile Basin (Aba Gerima, Guder and Dibatie)*; Final Project Report; Amhara Design and Supervision Works Enterprise: Bahir Dar, Ethiopia, 2016.
38. R Core Team. *R: A Language and Environment for Statistical Computing*; R Foundation for Statistical Computing: Vienna, Austria, 2020; Available online: https://www.R-project.org/ (accessed on 14 March 2023).
39. SCS. *National Engineering Handbook, Section 4. Hydrology*; Soil Conservation Service, US Department of Agriculture: Washington, DC, USA, 1972.
40. Hawkins, R.H.; Ward, T.J.; Woodward, D.E.; Van Mullem, J.A. *Curve Number Hydrology: State of the Practice*; American Society of Civil Engineers: Reston, WI, USA, 2008.
41. ESRI. *ArcGIS Pro (v2.6) Software*; Environmental Systems Research Institute (ESRI) Inc.: Redlands, CA, USA, 2020.
42. Neteler, M.; Mitasova, H. *Open Source GIS: A GRASS GIS Approach*; Springer Science & Business Media: Berlin/Heidelberg, Germany, 2013; Volume 689.
43. FDRE MoA. *Integrated Local Level Participatory Land Use Planning (ILLPLUP) Manual*; Rural Land Administration and Use Directorate (RLAUD): Addis Ababa, Ethiopia, 2020.
44. Evans, R.; Nortcliff, S. Soil erosion in north Norfolk. *J. Agric. Sci.* **1978**, *90*, 185–192. [CrossRef]
45. Speirs, R.B.; Frost, C.A. The increasing incidence of accelerated soil water erosion on arable land in the east of Scotland. *Res. Dev. Agric.* **1985**, *2*, 161–167.
46. Nachtergaele, J. A Spatial and Temporal Analysis of the Characteristics, Importance and Prediction of Ephemeral Gully Erosion. 2001. Available online: https://lirias.kuleuven.be/1737006?limo=0 (accessed on 14 March 2023).
47. Prosser, I.P.; Soufi, M. Controls on gully formation following forest clearing in a humid temperate environment. *Water Resour. Res.* **1998**, *34*, 3661–3671. [CrossRef]
48. Begin, Z.; Schumm, S. Instability of alluvial valley floors: A method for its assessment. *Trans. ASAE* **1979**, *22*, 347–0350. [CrossRef]
49. Geroy, I.; Gribb, M.; Marshall, H.-P.; Chandler, D.; Benner, S.G.; McNamara, J.P. Aspect influences on soil water retention and storage. *Hydrol. Process.* **2011**, *25*, 3836–3842. [CrossRef]
50. Svoray, T.; Michailov, E.; Cohen, A.; Rokah, L.; Sturm, A. Predicting gully initiation: Comparing data mining techniques, analytical hierarchy processes and the topographic threshold. *Earth Surf. Process. Landf.* **2012**, *37*, 607–619. [CrossRef]
51. Azareh, A.; Rahmati, O.; Rafiei-Sardooi, E.; Sankey, J.B.; Lee, S.; Shahabi, H.; Ahmad, B.B. Modelling gully-erosion susceptibility in a semi-arid region, Iran: Investigation of applicability of certainty factor and maximum entropy models. *Sci. Total Environ.* **2019**, *655*, 684–696. [CrossRef]
52. Javidan, N.; Kavian, A.; Pourghasemi, H.R.; Conoscenti, C.; Jafarian, Z. Gully erosion susceptibility mapping using multivariate adaptive regression splines—Replications and sample size scenarios. *Water* **2019**, *11*, 2319. [CrossRef]
53. Saha, S.; Roy, J.; Arabameri, A.; Blaschke, T.; Tien Bui, D. Machine learning-based gully erosion susceptibility mapping: A case study of Eastern India. *Sensors* **2020**, *20*, 1313. [CrossRef]
54. Jiang, C.; Fan, W.; Yu, N.; Liu, E. Spatial modeling of gully head erosion on the Loess Plateau using a certainty factor and random forest model. *Sci. Total Environ.* **2021**, *783*, 147040. [CrossRef] [PubMed]
55. Sidorchuk, A. Dynamic and static models of gully erosion. *Catena* **1999**, *37*, 401–414. [CrossRef]
56. Frankl, A.; Poesen, J.; Deckers, J.; Haile, M.; Nyssen, J. Gully head retreat rates in the semi-arid highlands of Northern Ethiopia. *Geomorphology* **2012**, *173*, 185–195. [CrossRef]
57. Herweg, K.; Ludi, E. The performance of selected soil and water conservation measures—Case studies from Ethiopia and Eritrea. *Catena* **1999**, *36*, 99–114. [CrossRef]
58. Adimassu, Z.; Langan, S.; Johnston, R.; Mekuria, W.; Amede, T. Impacts of soil and water conservation practices on crop yield, run-off, soil loss and nutrient loss in Ethiopia: Review and synthesis. *Environ. Manag.* **2017**, *59*, 87–101. [CrossRef] [PubMed]
59. Wolka, K.; Biazin, B.; Martinsen, V.; Mulder, J. Soil and water conservation management on hill slopes in Southwest Ethiopia. I. Effects of soil bunds on surface runoff, erosion and loss of nutrients. *Sci. Total Environ.* **2021**, *757*, 142877. [CrossRef]